

# Unravelling electrical structure of the mantle with ionospheric, magnetospheric and oceanic sources

**Alexander Grayver**

Institute of Geophysics and Meteorology, University of Cologne

Institute of Geophysics, ETH Zurich

Electromagnetic Induction Workshop 2022, Review talk

# Deep Electromagnetic sounding is a (very) old technique!

## XV. *The Diurnal Variation of Terrestrial Magnetism.*

By ARTHUR SCHUSTER, *F.R.S., Professor of Physics in Owens College.* With an  
*Appendix* by H. LAMB, *F.R.S., Professor of Mathematics in Owens College.*

Received March 20,—Read March 28, 1889.

believe to be of importance. The results of the calculation point not only to an external source, but to an additional internal source, standing in fixed relationship to the external cause. This we might have expected. A varying potential due to external causes must be accompanied by currents induced in the Earth's body, which, in turn, must affect the magnetic needle. The phase of these currents and their magnitude lead us to form definite conclusions on the average conducting power of the Earth, and it will be seen that there is strong evidence that the average conductivity is very small near the surface, but must be greater further down. In this part of the investigation I had much assistance from my colleague, Professor LAMB.

The first paper on GDS was published 133 years ago!

Long before any other EM/electric method was established or practiced.

Before plate tectonics was proposed or inner/outer core was discovered...

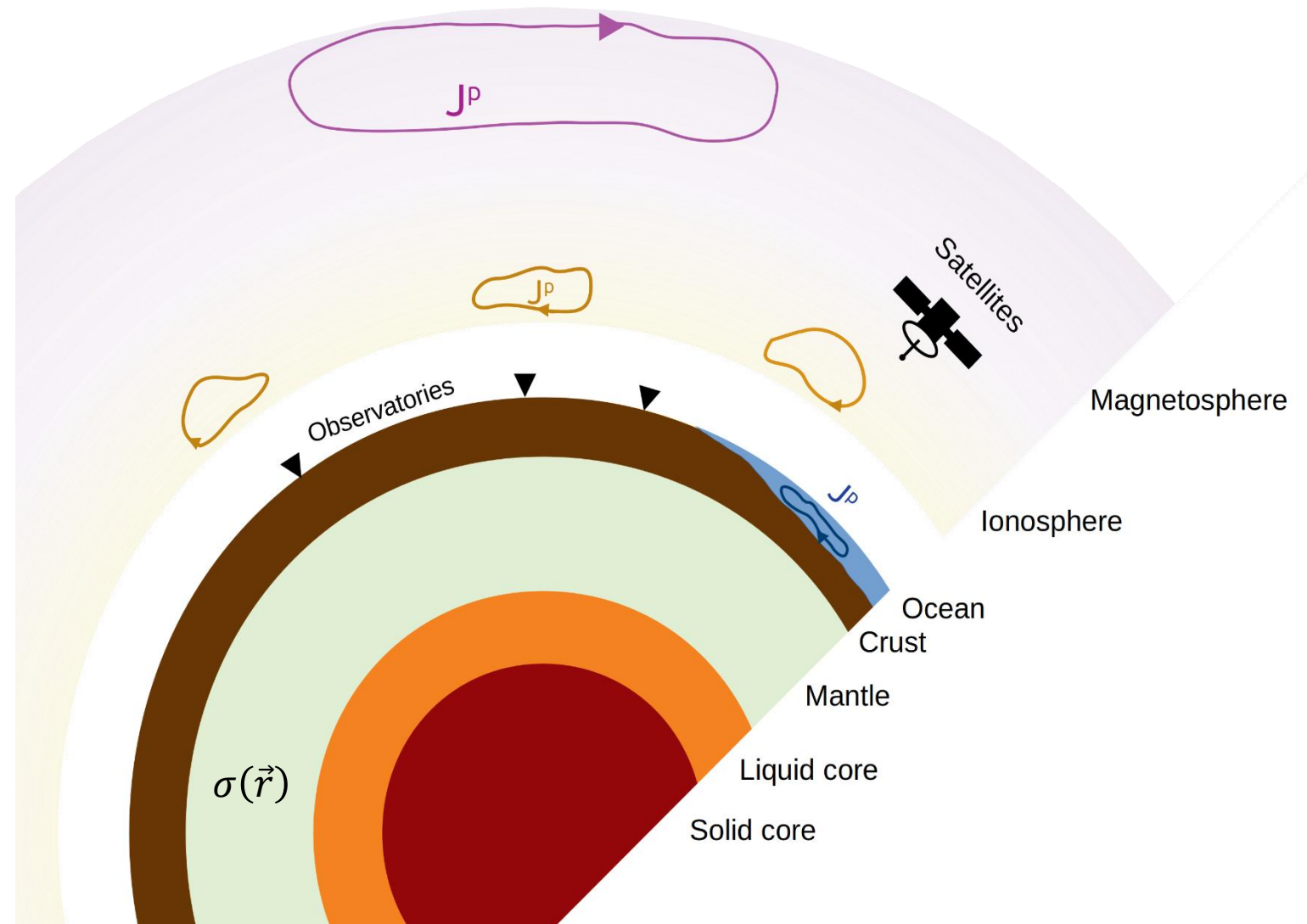
# Scope and past reviews

Year of the review talk	Title	Reference
1972	Global electrical conductivity of the Earth	<a href="#">Rikitake (1973)</a>
1972	The theory of geomagnetic induction	<a href="#">Price (1973)</a>
1972	Global electromagnetic induction in the moon and planets	<a href="#">Dyal and Parkin (1973)</a>
1972	Global geomagnetic sounding - methods and results	<a href="#">Bailey (1973)</a>
1974	Morphology of slowly-varying geomagnetic external fields - A review	<a href="#">Matsushita (1975)</a>
1974	On the inversion of global electromagnetic induction data	<a href="#">Anderssen (1975)</a>
1974	Analytical solutions to global and local problems of electromagnetic induction in the Earth	<a href="#">Hobbs (1975)</a>
1974	Solar-wind induction and lunar conductivity	<a href="#">Sonett (1975)</a>
1978	The electrical conductivity of the moon	<a href="#">Vanyan (1980)</a>
1984	Global electromagnetic induction	<a href="#">Roberts (1986)</a>
1986	The global conductivity distribution	<a href="#">Parkinson (1988)</a>
1998	Induction studies with satellite data	<a href="#">Olsen (1999)</a>
2010	Deep electromagnetic studies from land, sea, and space: Progress status in the past 10 years	<a href="#">Kuvshinov (2012)</a>
2022	Unravelling the Electrical Conductivity of Earth and Planets – A review	This paper

- *This review will cover years from 2012 to present*
- *Spatial scales from  $10^3$  km to the global*
- *Space weather / GICs won't be covered*
- *Planetary studies will not be included (next review?)*

# Electromagnetic (EM) induction methods

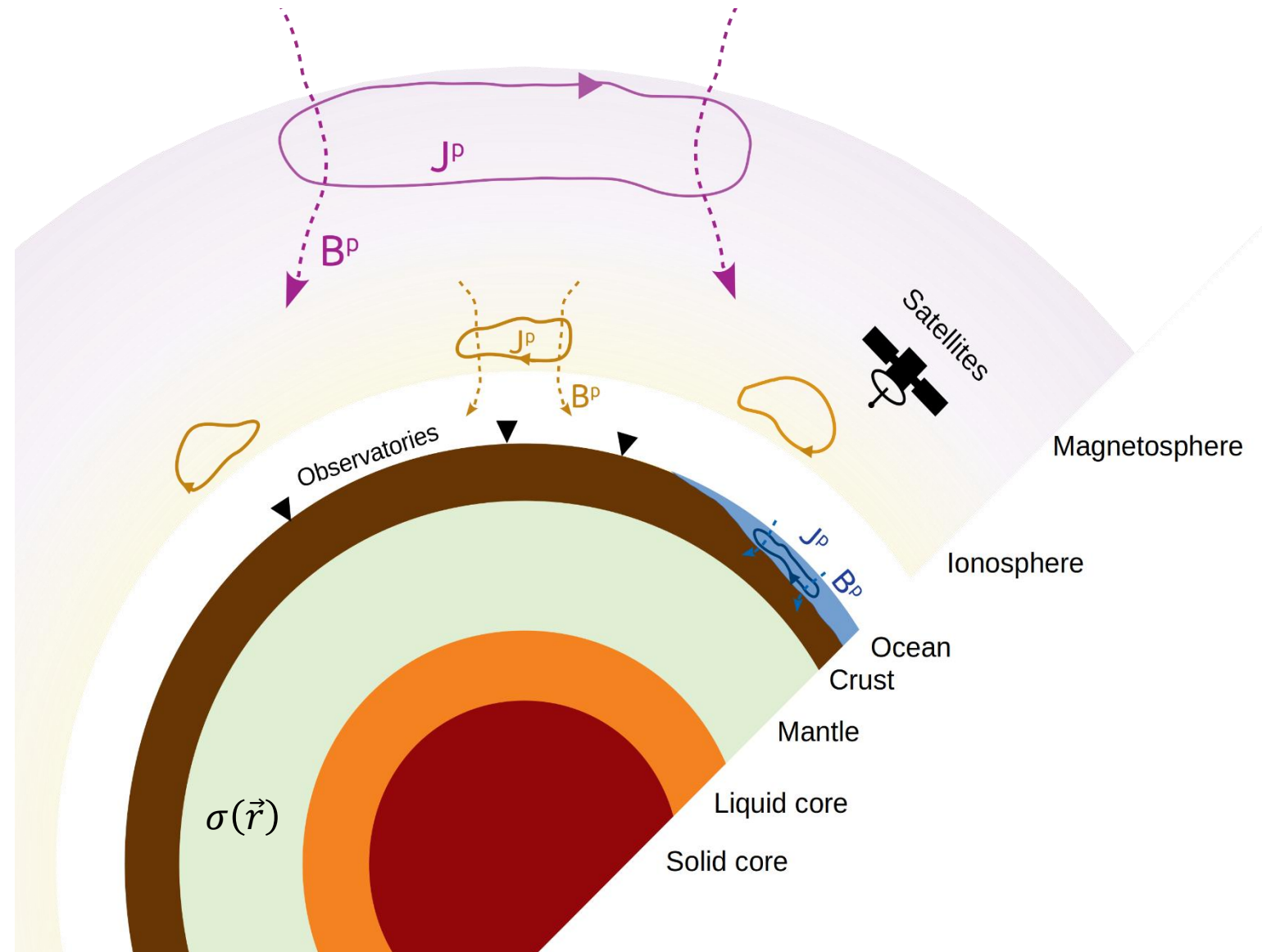
- EM methods measure the Earth response to a *time-varying* EM source field.
- The EM response depends on subsurface *conductivity* structure
- $J^p$  – primary electric currents
- $B^p$  – primary magnetic field
- $J^s$  – secondary electric currents
- $B^s$  – secondary magnetic field





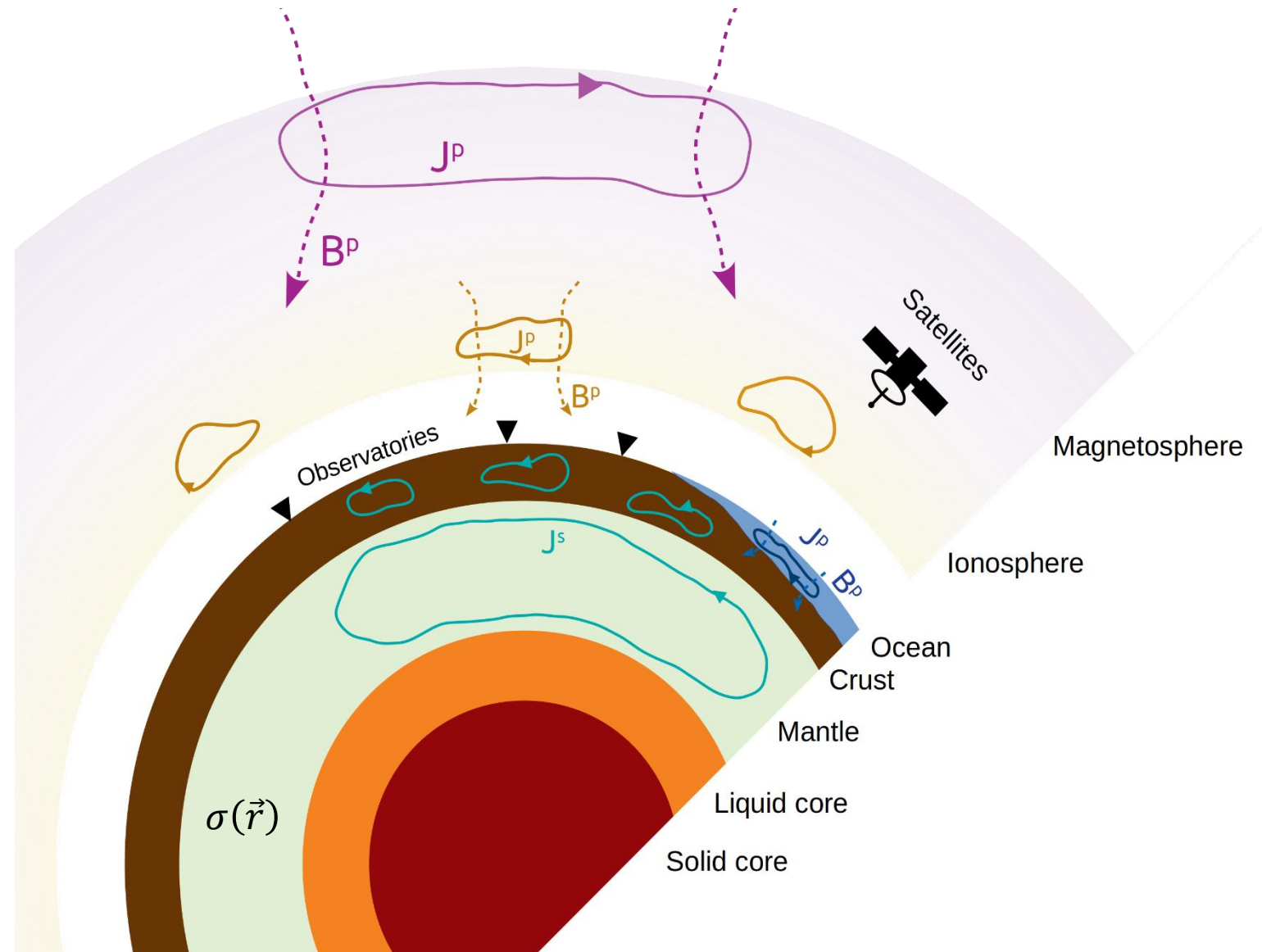
# Electromagnetic (EM) induction methods

- EM methods measure the Earth response to a *time-varying* EM source field.
- The EM response depends on Earth's conductivity structure
- $J^p$  – primary electric currents
- $B^p$  – primary magnetic field
- $J^s$  – secondary electric currents
- $B^s$  – secondary magnetic field



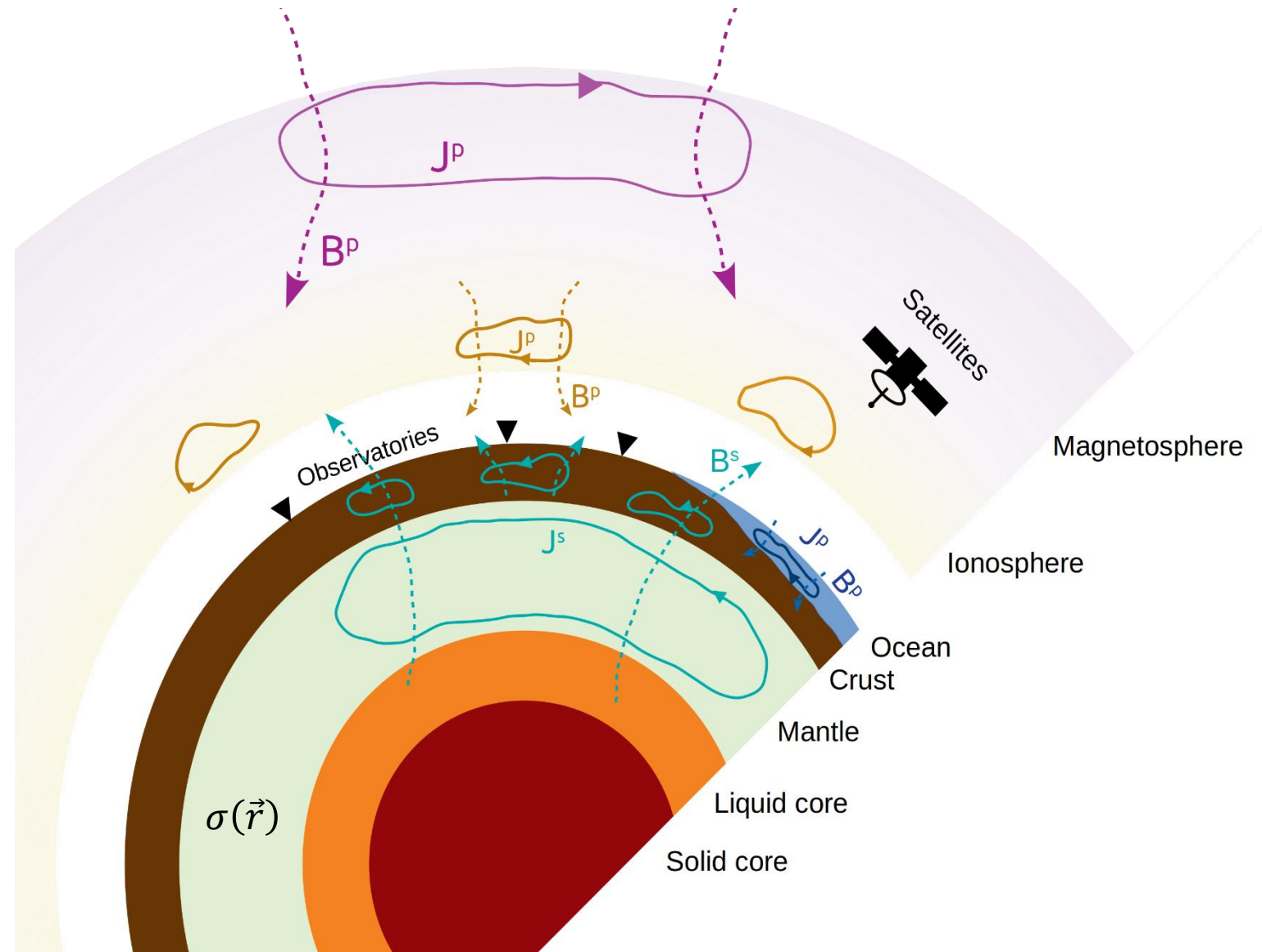
# Electromagnetic (EM) induction methods

- EM methods measure the Earth response to a *time-varying* EM source field.
- The EM response depends on Earth's conductivity structure
- $J^p$  – primary electric currents
- $B^p$  – primary magnetic field
- $J^s$  – secondary electric currents
- $B^s$  – secondary magnetic field



# Electromagnetic (EM) induction methods

- EM methods measure the Earth response to a *time-varying* EM source field.
- The EM response depends on Earth's conductivity structure
- $J^p$  – primary electric currents
- $B^p$  – primary magnetic field
- $J^s$  – secondary electric currents
- $B^s$  – secondary magnetic field

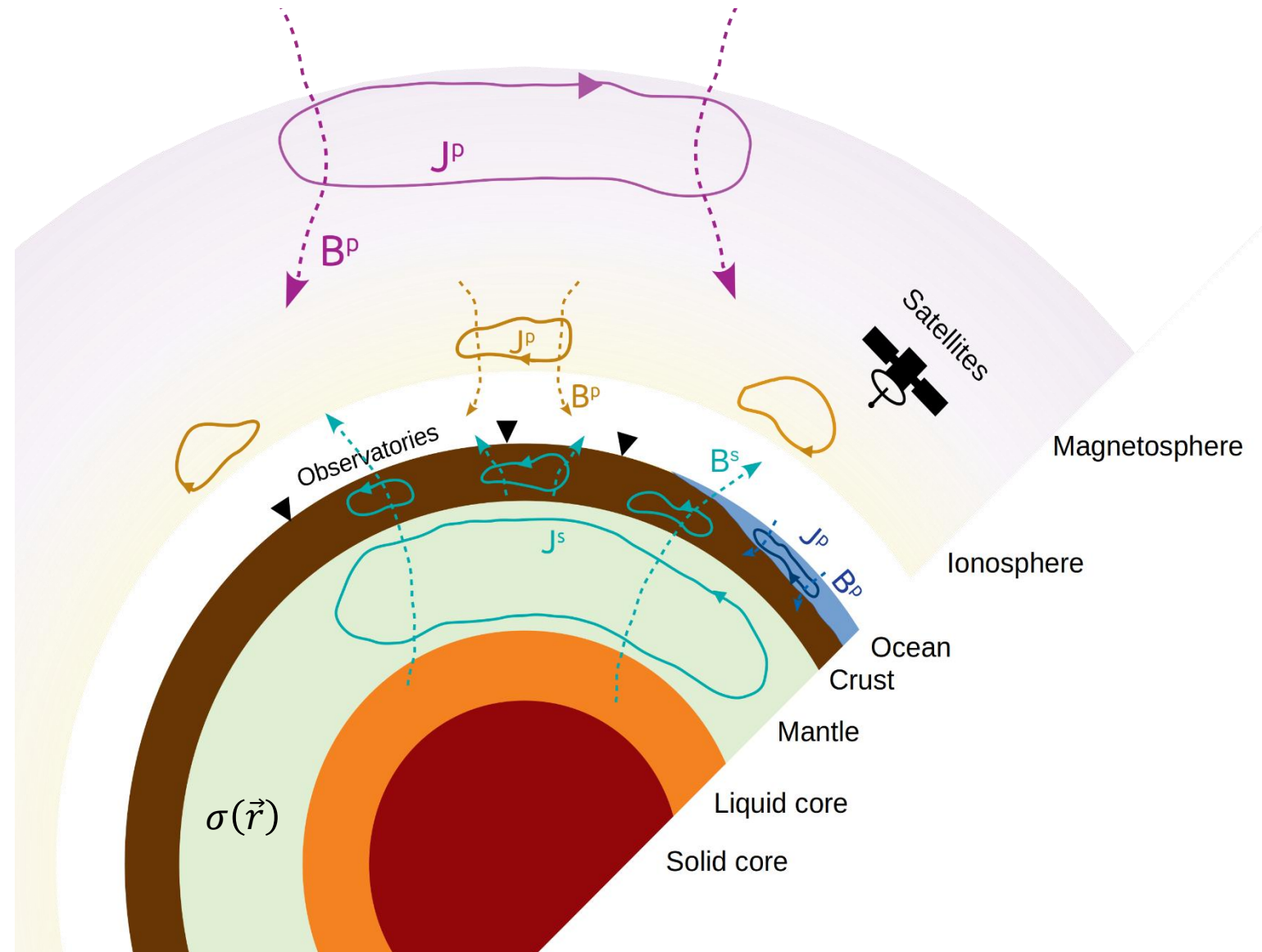


# Electromagnetic (EM) induction methods

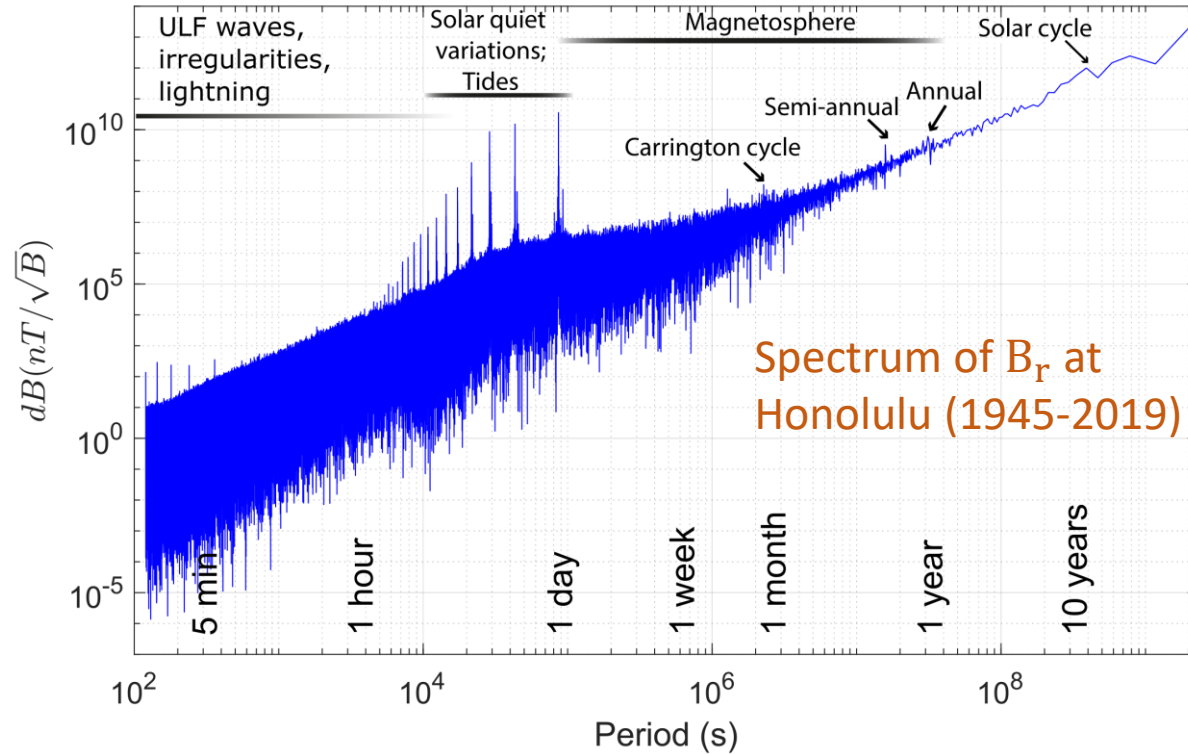
- EM methods measure the Earth response to a *time-varying* EM source field.
- The EM response depends on Earth's conductivity structure
- Governing equations:

$$\mu^{-1} \nabla \times \vec{B} = \sigma \vec{E} + \vec{j}^p$$

$$\nabla \times \vec{E} = -\frac{\partial \vec{B}}{\partial t}$$

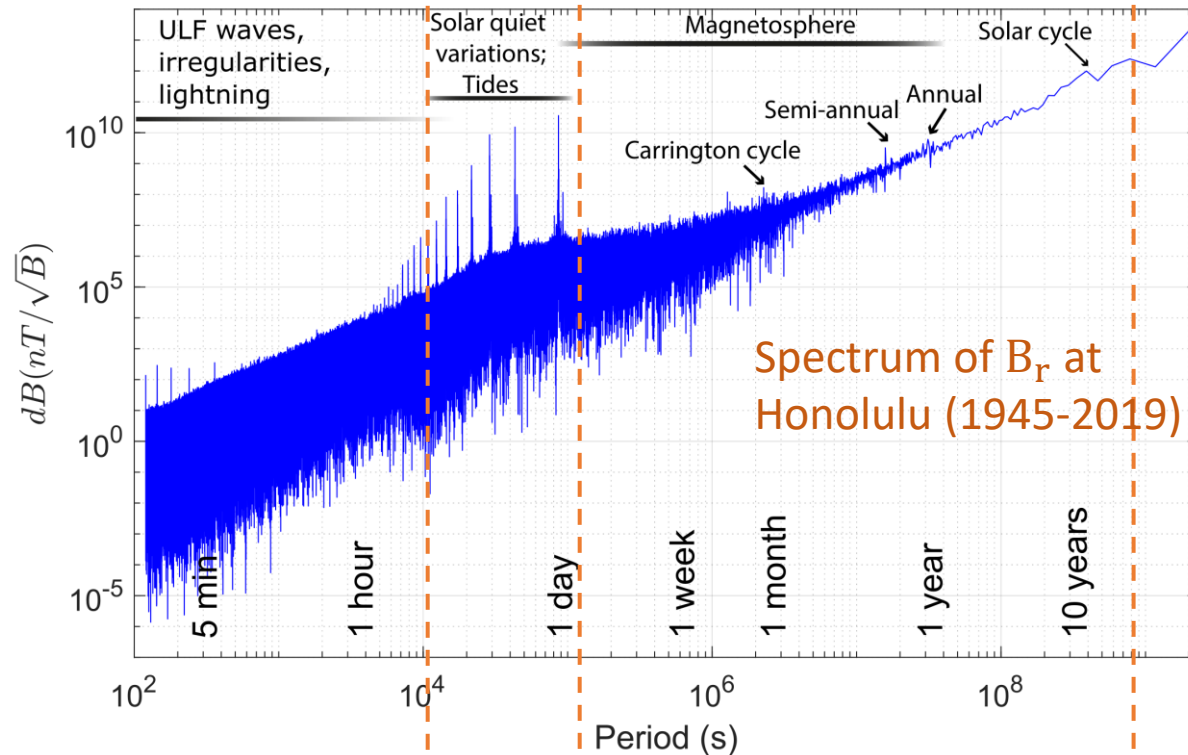


# Earth's electromagnetic environment





# Earth's electromagnetic environment

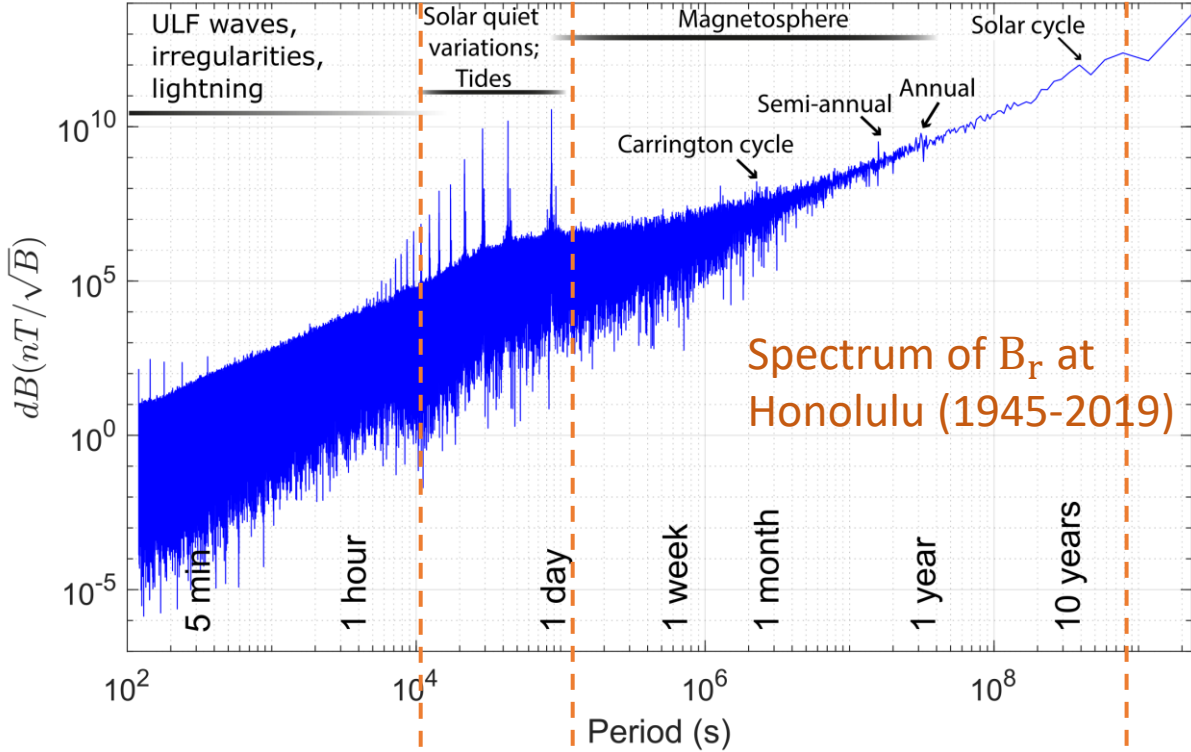


- Depth of sounding is proportional to the period.
- Simple “plane wave” source assumption at shorter periods.
- Complex and heterogeneous sources at longer periods. Source structure is generally not known.

Band: “Plane wave” “Daily” “Magnetospheric”

Depth (km): < 350 200-600 > 400 (down to CMB)

# Earth's electromagnetic environment



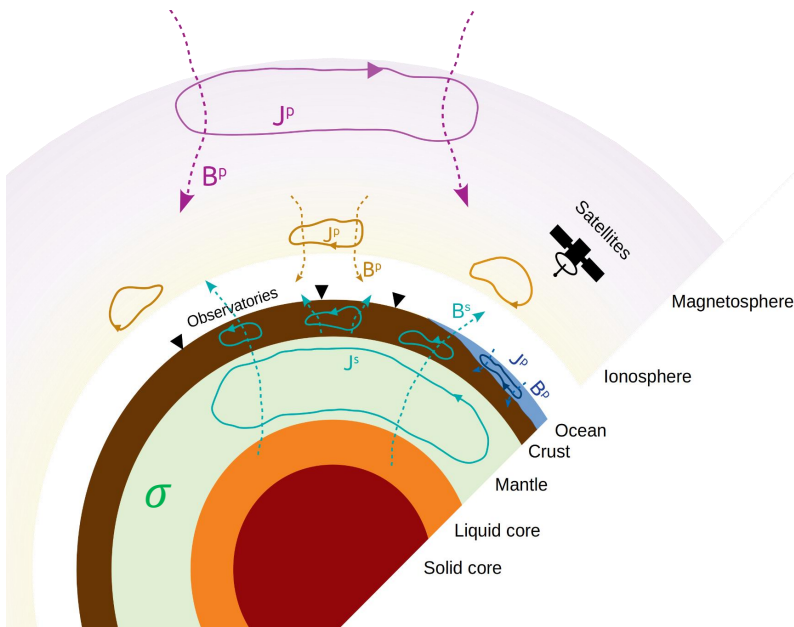
Band:	“Plane wave”	“Daily”	“Magnetospheric”
Depth (km):	< 350	200-600	> 400 (down to CMB)
Inversion strategy:	(1)	(1), (2)	(2)

Magnetotelluric / Oceanic tidal sources:

$$(1) \min_{\sigma} \|d - F(\sigma)\|_2^2 + R(\sigma)$$

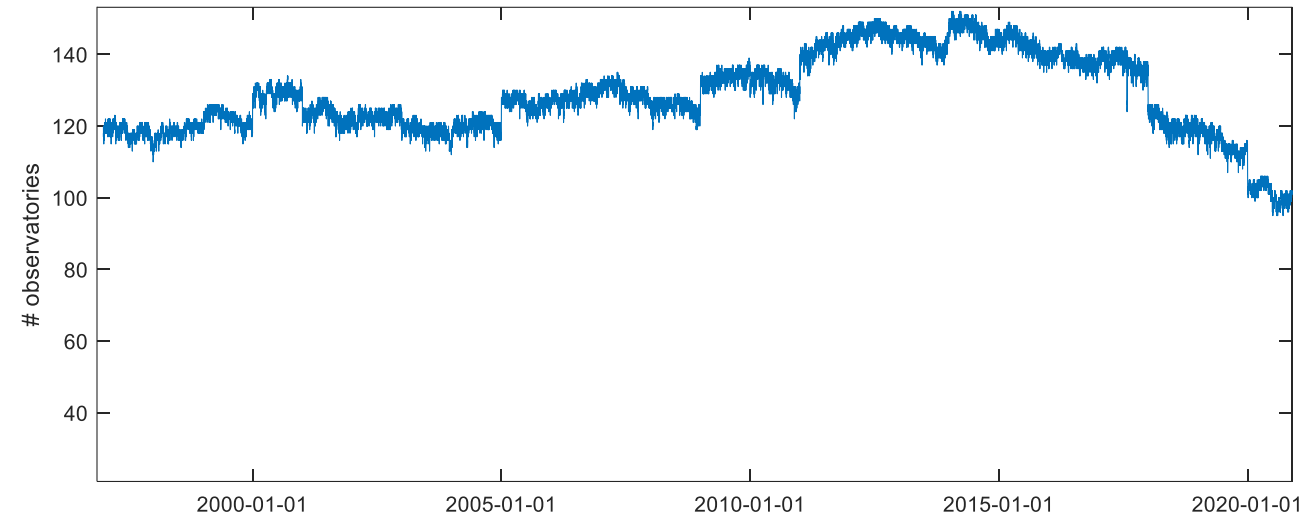
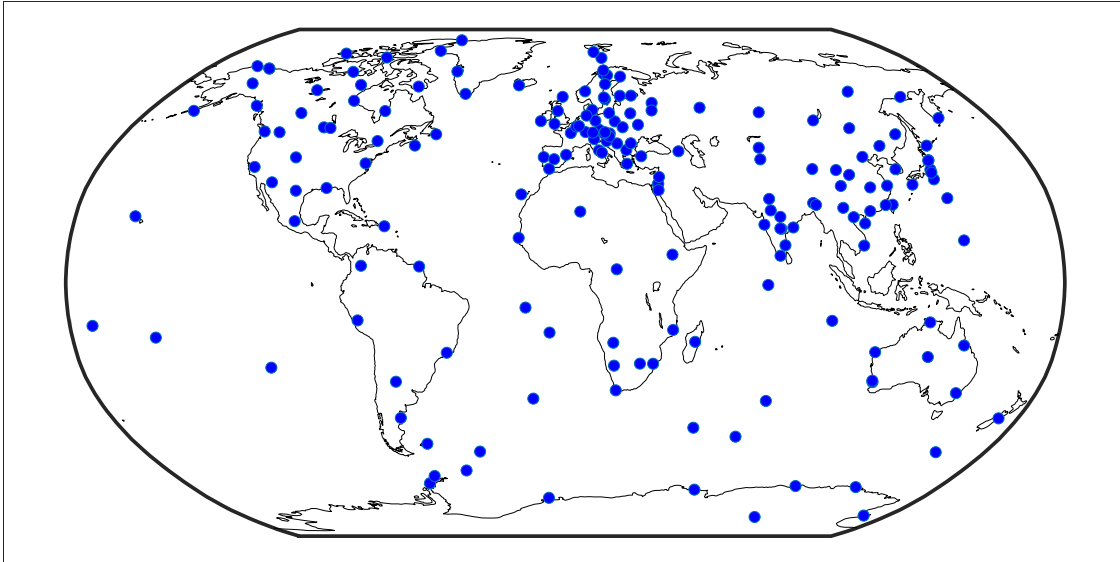
Long-period Ionospheric / Magnetospheric sources:

$$(2) \min_{\sigma, j^p} \|d - F(\sigma)j^p\|_2^2 + R(\sigma, j^p)$$



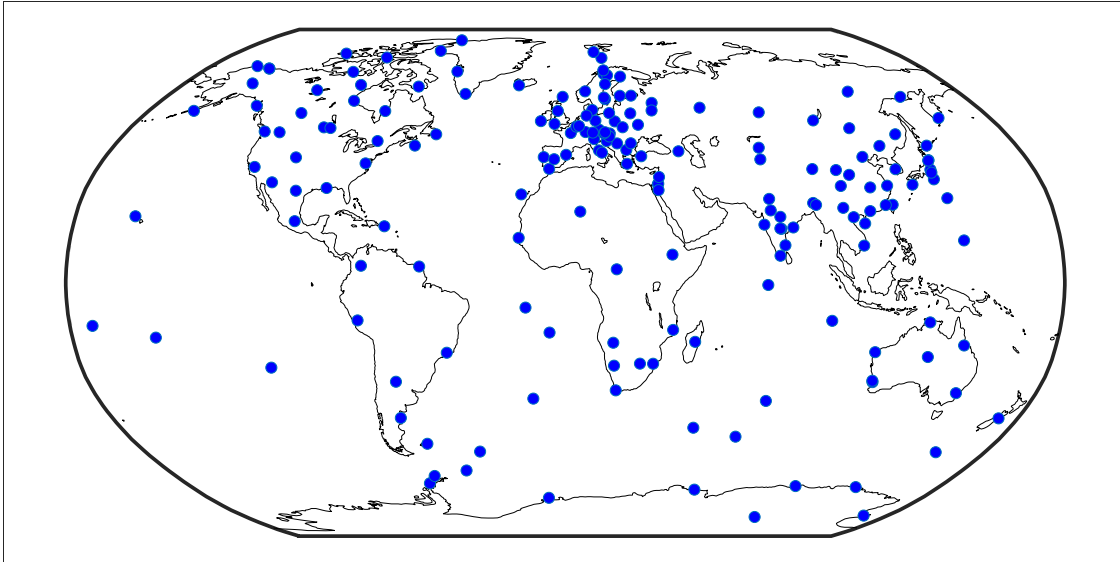
# Data

# Data: geomagnetic observatories



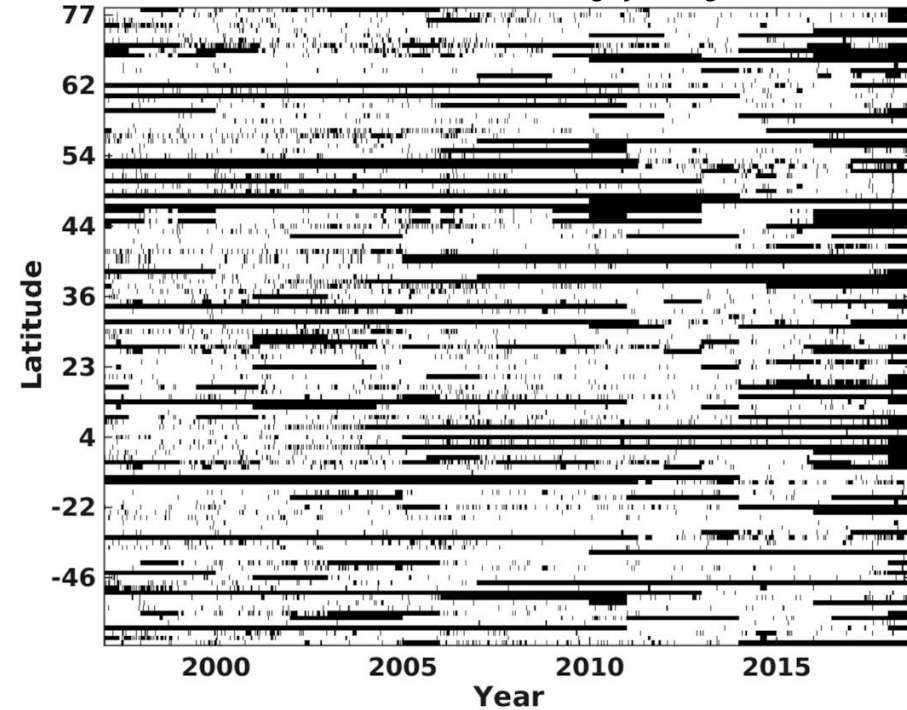
MacMillan and Olsen 2013: maintained BGS product (hourly, minute, second data) based on INTERMAGNET and other sources

# Data: geomagnetic observatories



Black indicates gaps

*Image from Egbert et al 2021*

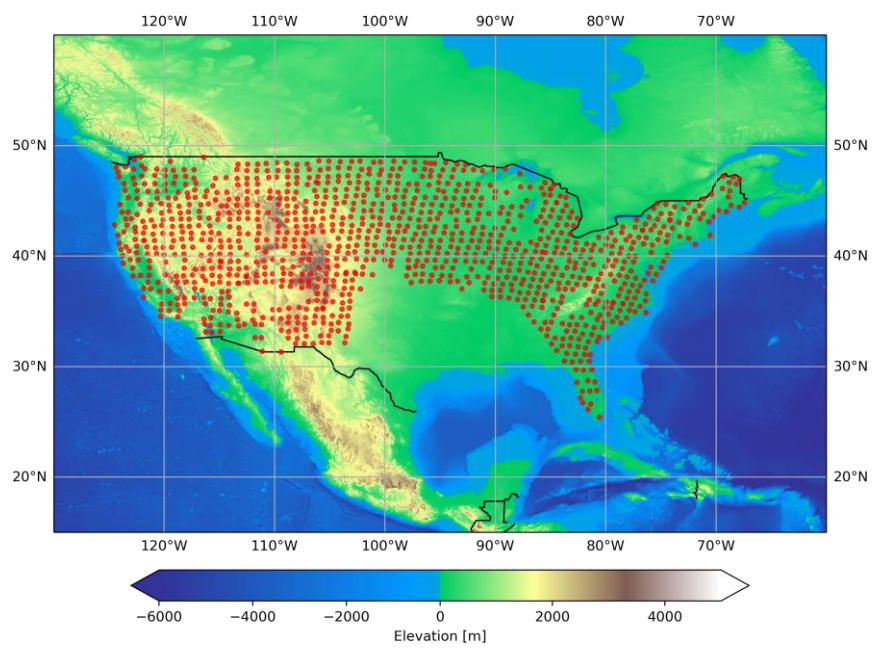


MacMillan and Olsen 2013: maintained BGS product (hourly, minute, second data) based on INTERMAGNET and other sources



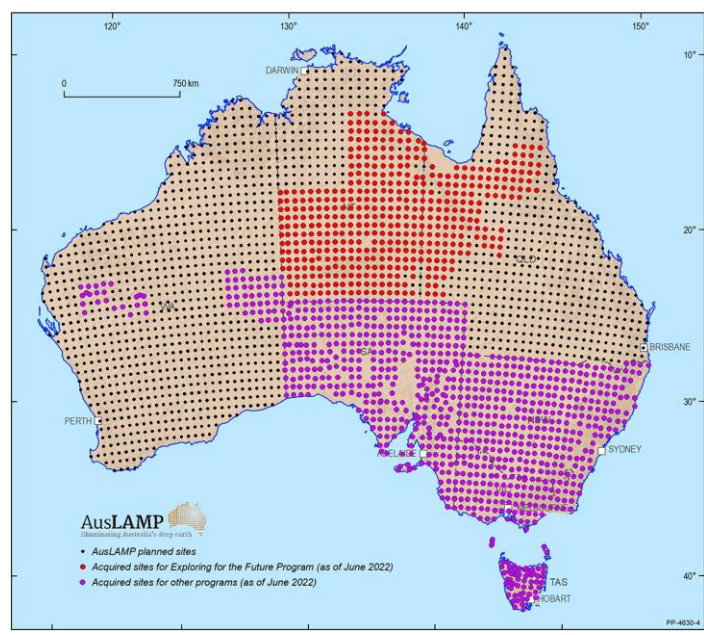
# Data: large-scale arrays

USArray



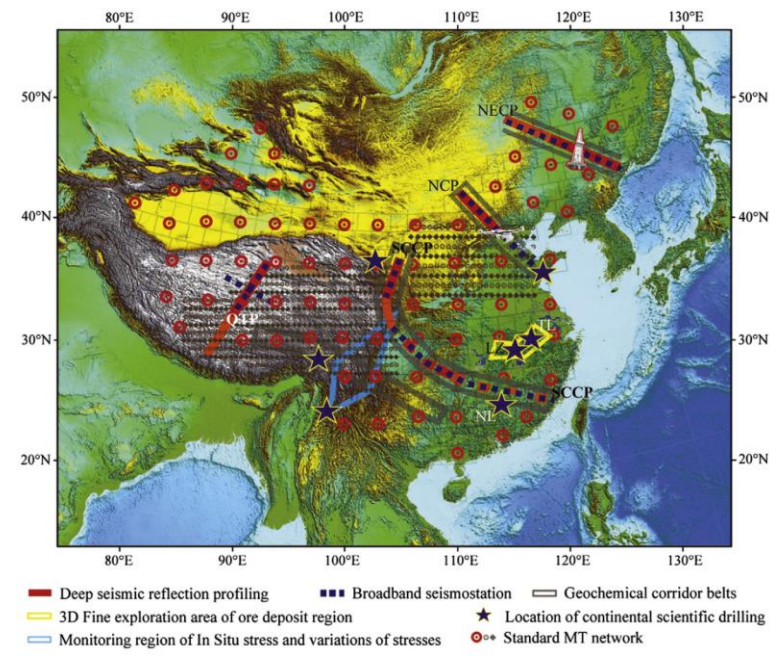
Schultz et al. 2006 – 2022, OSU, USGS

AusLAMP



Geoscience Australia, 2022

SinoProbe



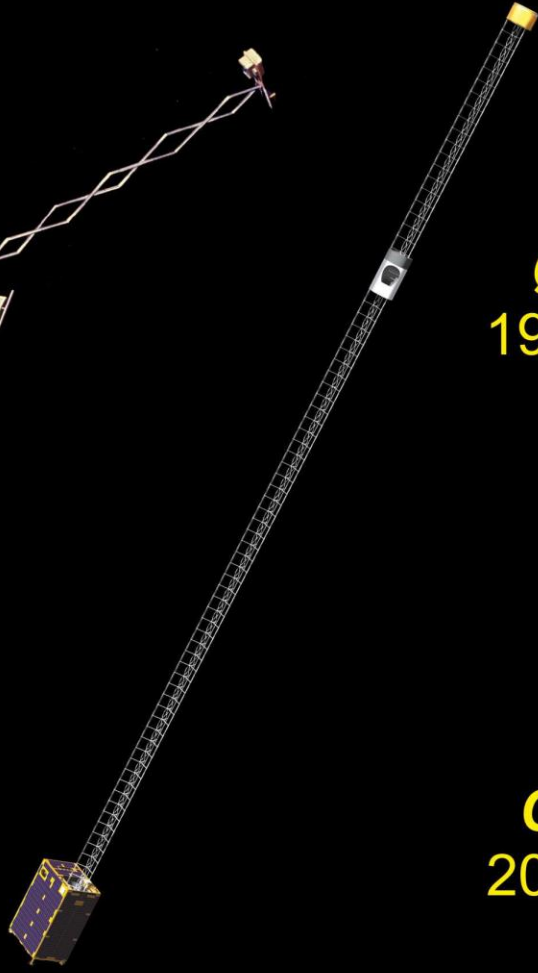
Dong et al., 2022



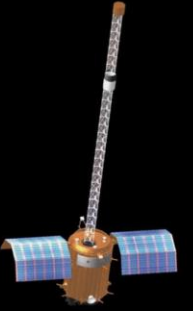
**POGO**  
1965-70



**MAGSAT**  
1979-80



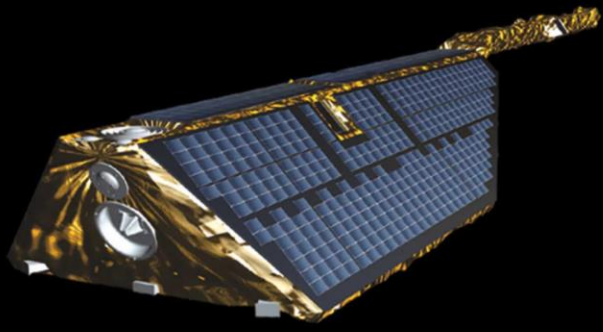
**Ørsted**  
1999-2014



**SAC-C**  
2000-2005

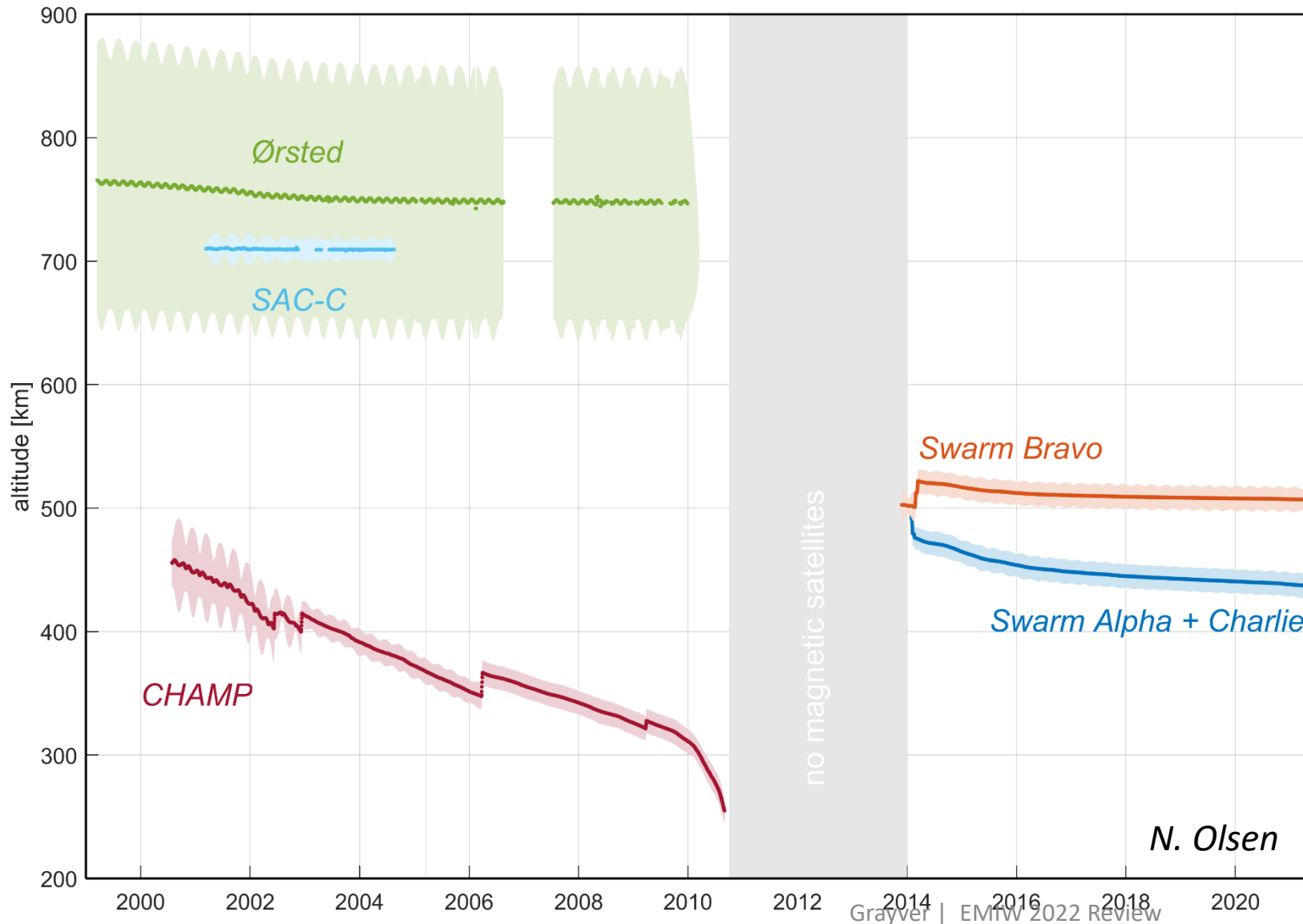


**Swarm**  
2013-



**CHAMP**  
2000-2010

# Data: Dedicated Science Satellites

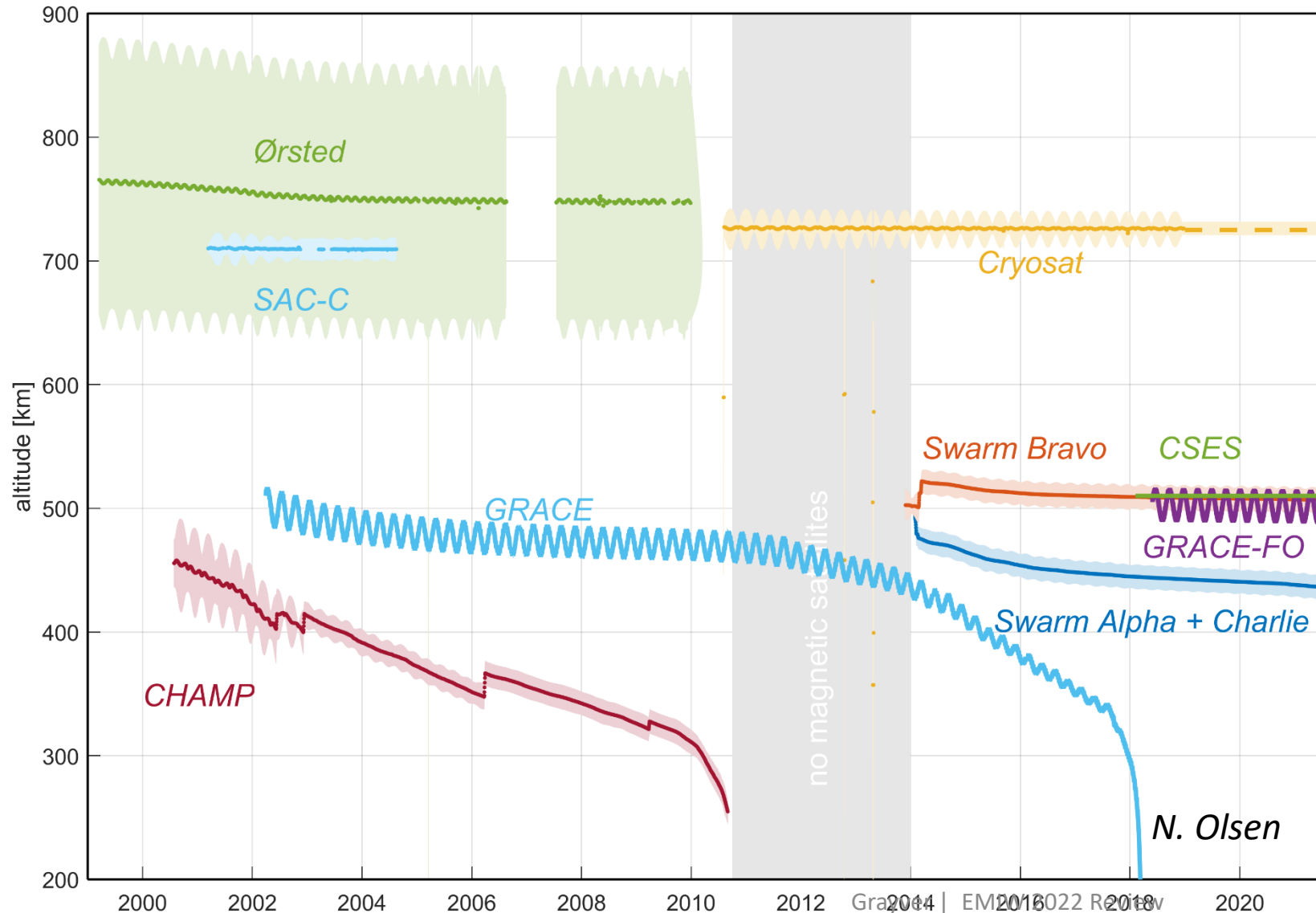


No high-precision magnetic field data are available in the gap between CHAMP and Swarm (Oct 2010 and Nov 2013)

*N. Olsen*



# Data: Dedicated Science Satellites + Platform Magnetometers



No high-precision magnetic field data are available in the gap between CHAMP and Swarm (Oct 2010 and Nov 2013)

Swarm, GRACE-FO and CryoSat-2 provide simultaneous data for improved time-space separation of external sources

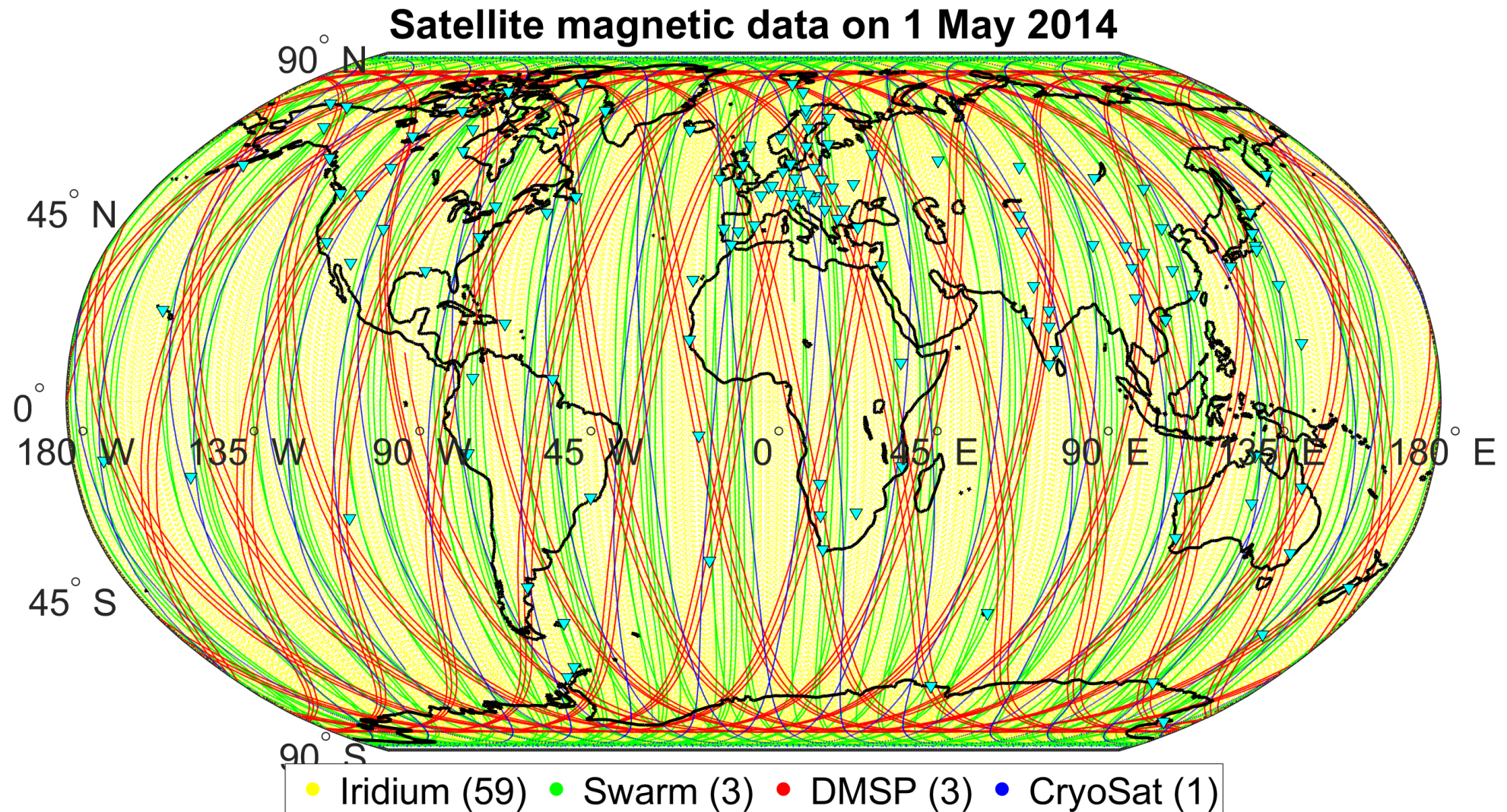
Swarm: Olsen et al. 2013

CSES: Shen et al. 2018

CryoSat-2: Olsen et al. 2020

GRACE-FO: Stolle et al. 2021

# Data: Dedicated Science Satellites + Platform Magnetometers





# Data: summary

- **Geomagnetic observatories**

- **Pros:** long quality-controlled time series
- **Cons:** uneven sparse coverage

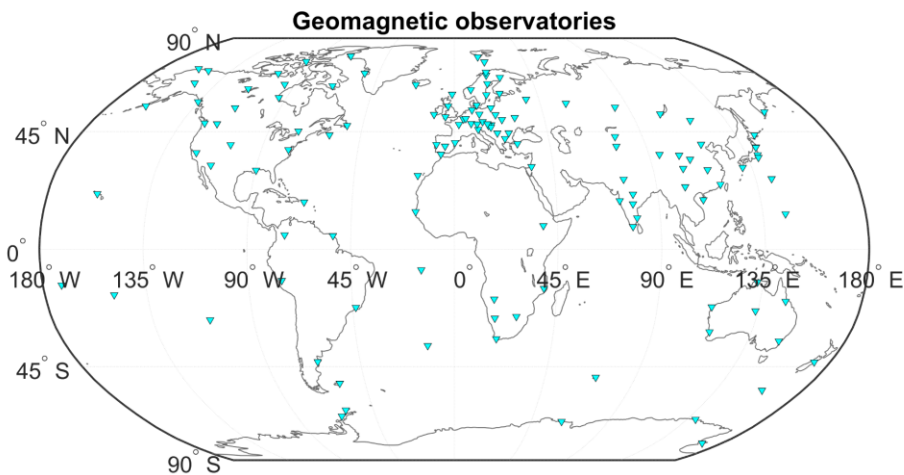
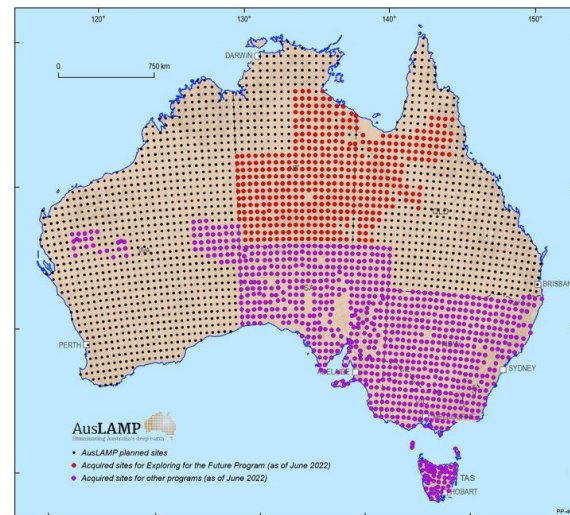


Image: GFZ

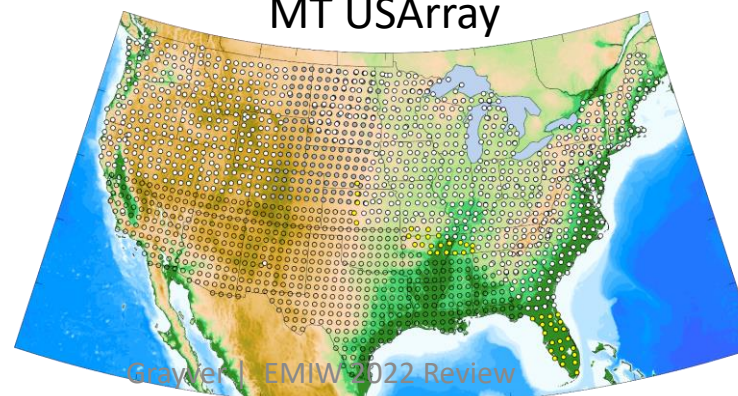
- **Temporary stations (arrays)**

- **Pros:** improved local resolution
- **Cons:** short time series

## AusLAMP



## MT USArray



- **Satellites** (CHAMP 2000-2010, Swarm 2013 - present)

- **Pros:** accuracy, coverage
- **Cons:** space-time aliasing



ESA Swarm satellites

- **New:** satellite platform magnetometers (potentially hundreds of satellites, e.g. CryoSat-2, GRACE-FO)
- **Pros:** unprecedented resolution
- **Cons:** lower accuracy (1x – 100x nT)

# Modelling and Inversion

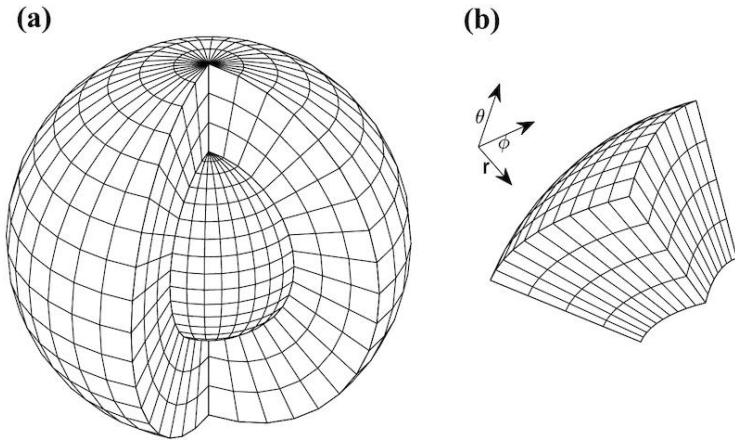
# Modelling and inversion

- Modelling benchmark study by Kelbert et al. 2014:
  - Tested 7 codes
  - Many new codes since then...
- FD: Zhang et al. 2019 (ModEM-based)
- FE: Grayver et al. (2019); Yao et al. (2022)
- IE: Chen et al. 2021; Kruglyakov and Kuvshinov 2022
- Spectral-FE: Velimsky et al. 2018 (frequency domain), Velimsky et al. 2019 (TD)
- Derivation of general adjoint operators (essential for 3-D inversion):
  - Egbert and Kelbert 2012
  - Pankratov and Kuvshinov 2010, 2014

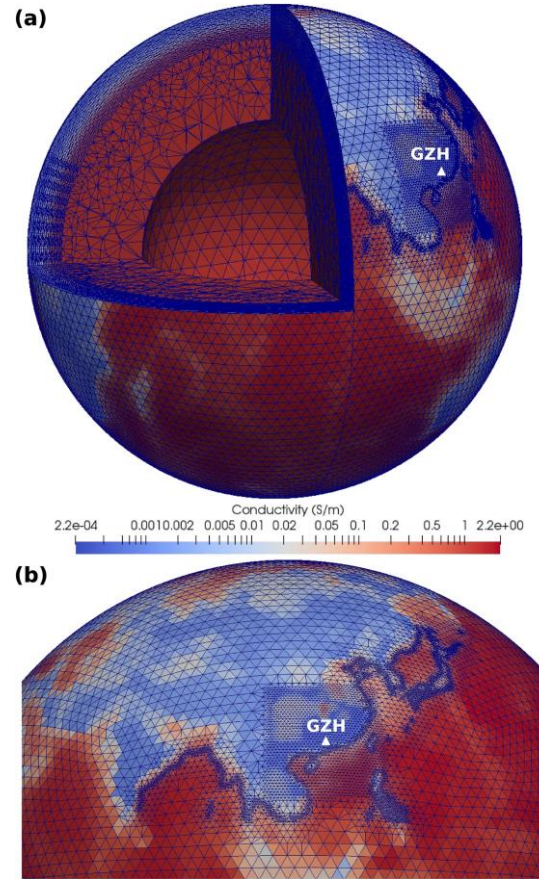


# Multi-scale grids and regional modelling

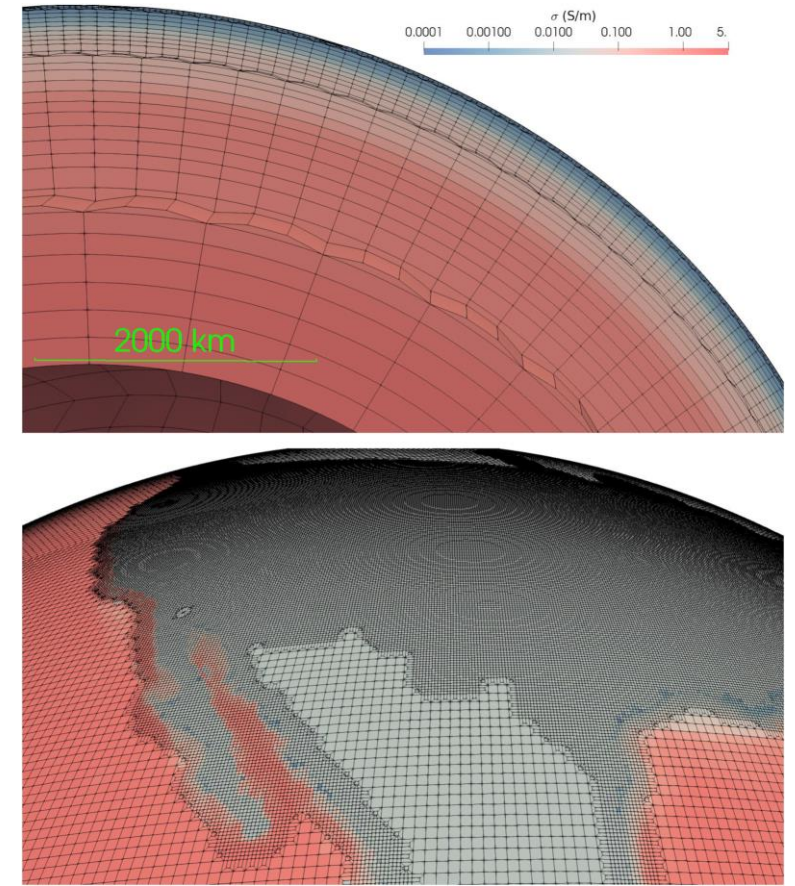
Zhang et al. 2019 (ModEM)



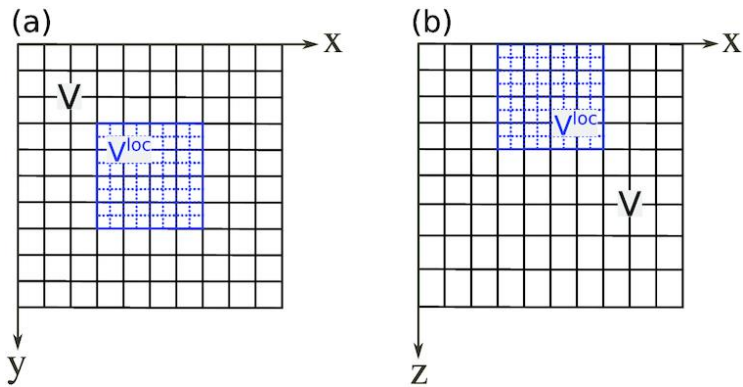
Yao et al. 2022



Grayver et al. 2019



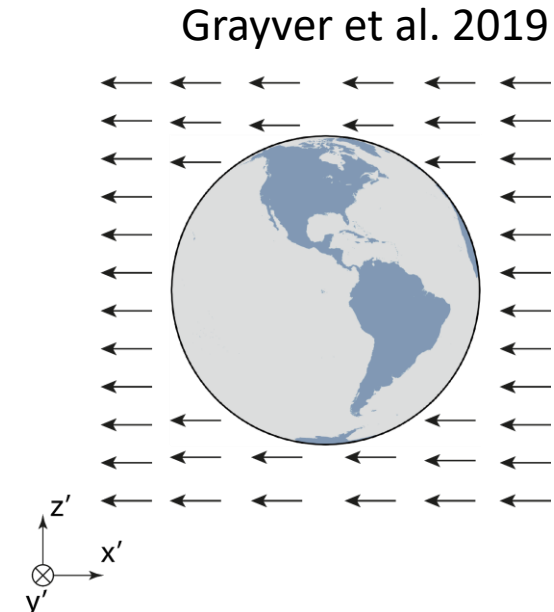
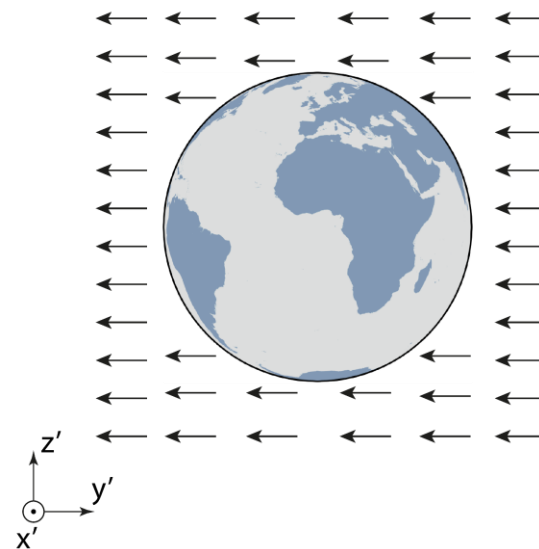
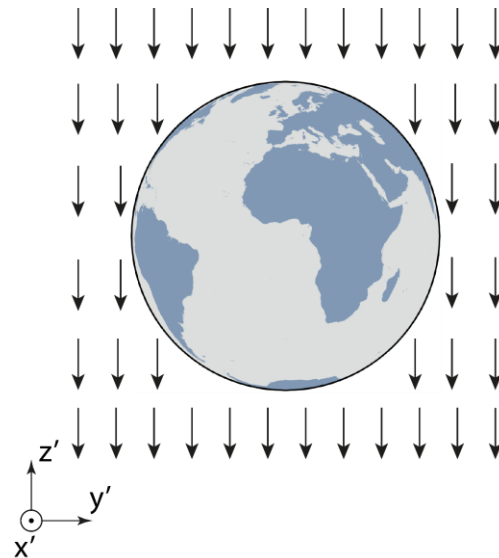
Chen et al. 2022 (Nested-IE)



# 3-D MT modelling in a sphere

- Uniform planetary fields (Fainberg et al. 1983).
- Described by degree 1 Spherical Harmonic functions.
- Reproduces plane wave impedance in a relevant period range.
- No tippers due to non-zero  $B_r$ .

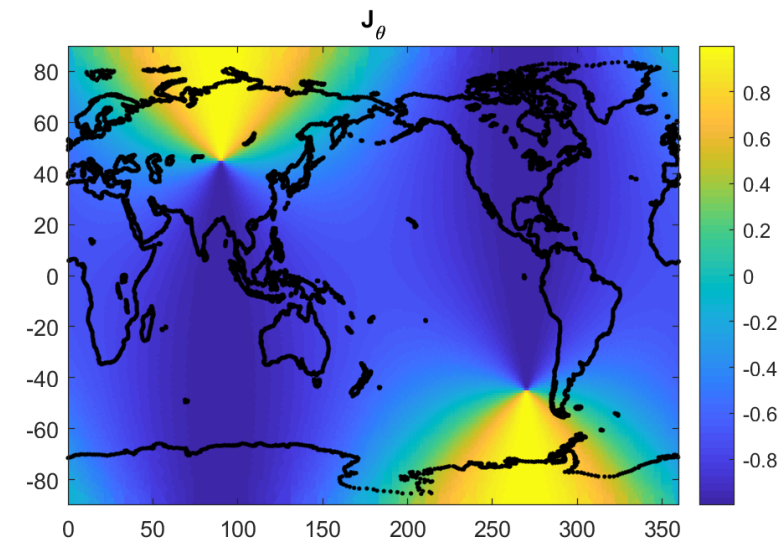
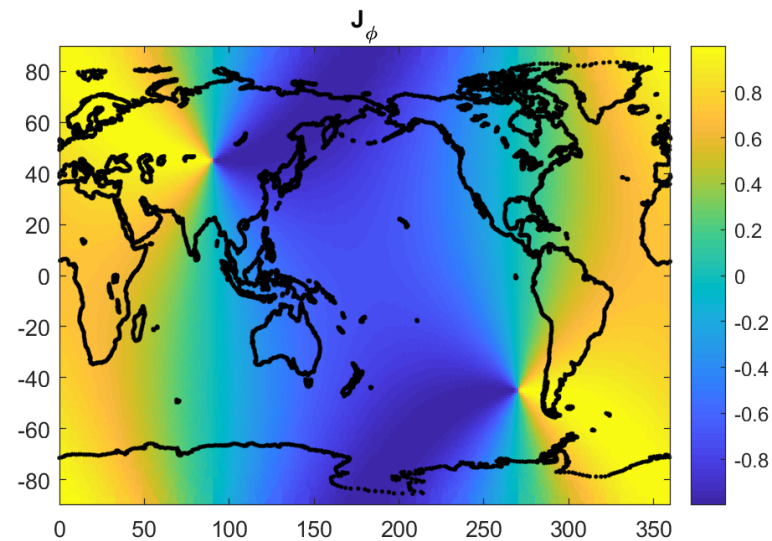
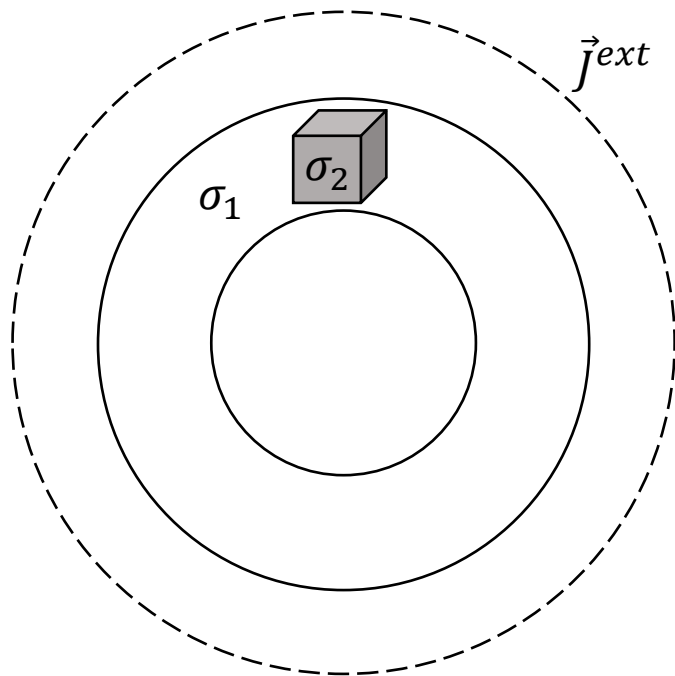
$$= \begin{bmatrix} Z_{xx} & Z_{xy} \\ Z_{yx} & Z_{yy} \end{bmatrix} \begin{bmatrix} -E_{\theta}^1 & -E_{\theta}^2 & -E_{\theta}^3 \\ E_{\phi}^1 & E_{\phi}^2 & E_{\phi}^3 \\ -H_{\theta}^1 & -H_{\theta}^2 & -H_{\theta}^3 \\ H_{\phi}^1 & H_{\phi}^2 & H_{\phi}^3 \end{bmatrix}$$



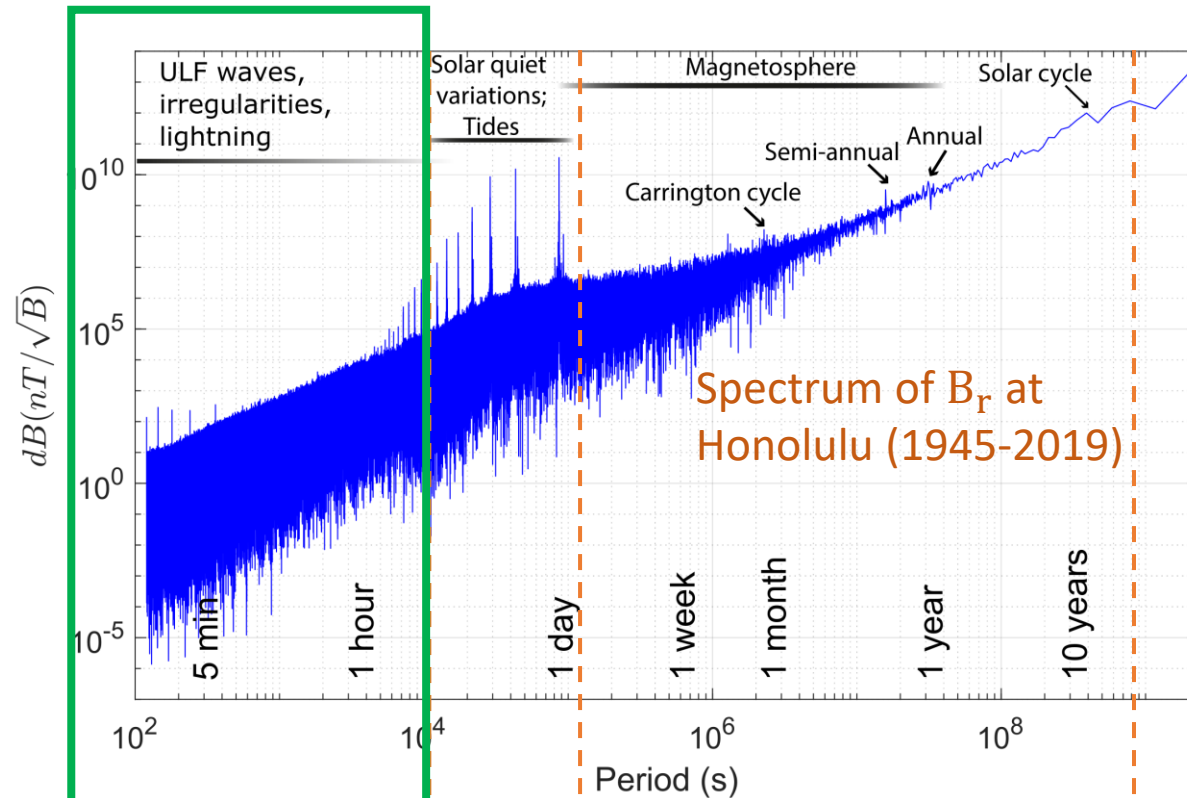


# 3-D MT modelling in a sphere

- Alternative source model based on a sheet current  $\vec{j}^{ext}$  flowing in  $\vartheta$ -direction placed above the Earth's surface + plus two rotated orthogonal polarizations (Kruglyakov and Kuvshinov, 2022).
- Radial (vertical) field is zero for any 1-D model, thus it can be used to compute tippers.



# Large-scale MT / GDS

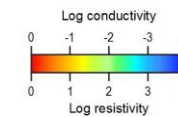
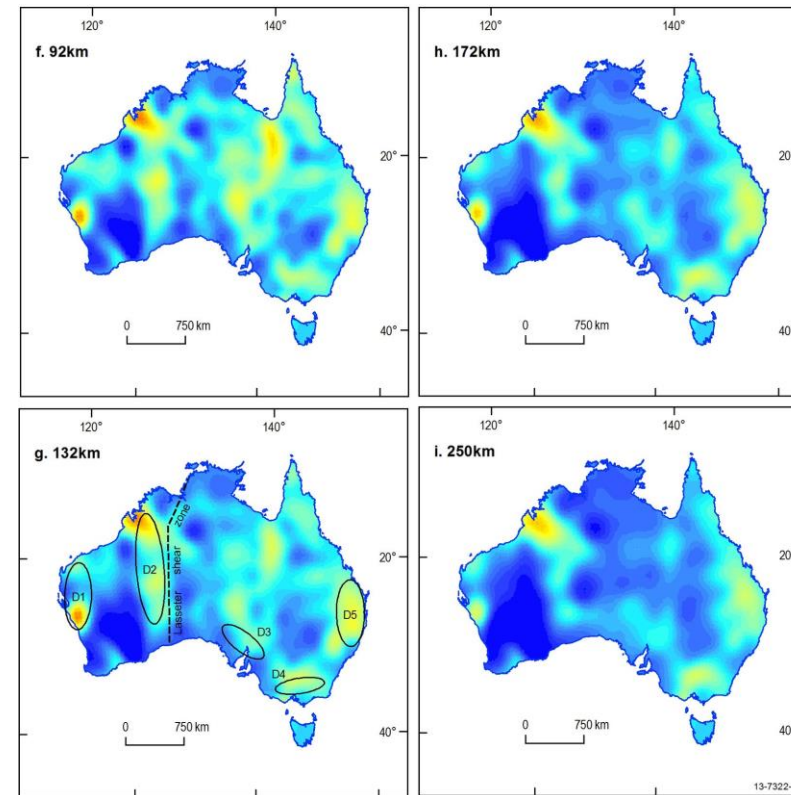
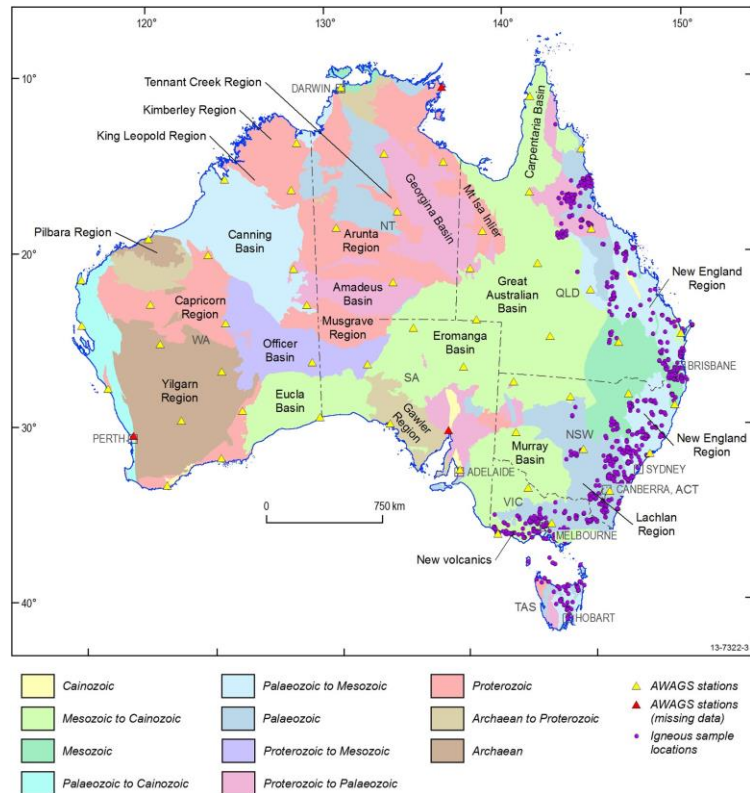


Spectrum of  $B_r$  at Honolulu (1945-2019)

Band: "Plane wave" "Daily" "Magnetospheric"

Sounding depth (km): < 350 200-500 > 400

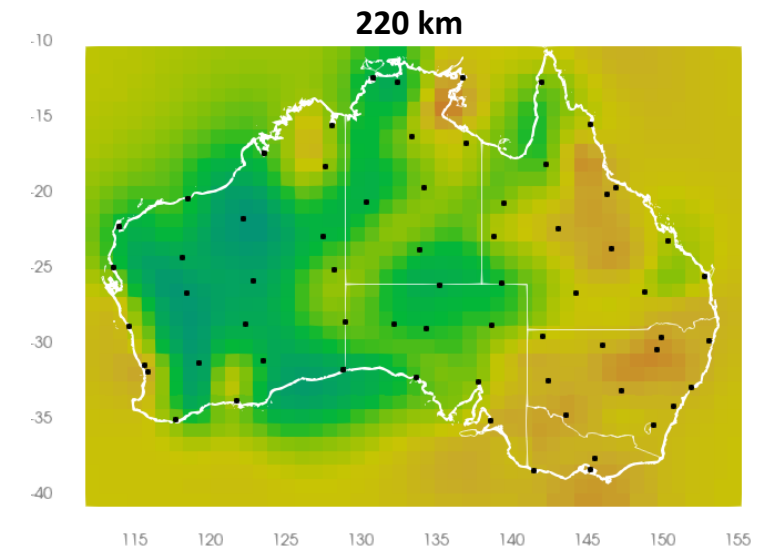
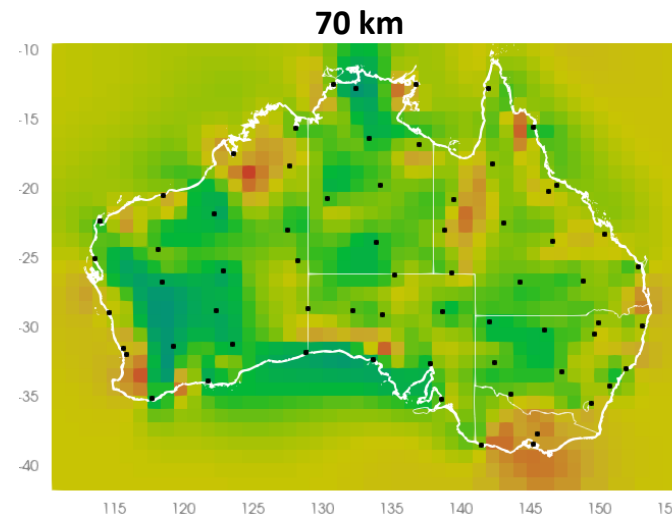
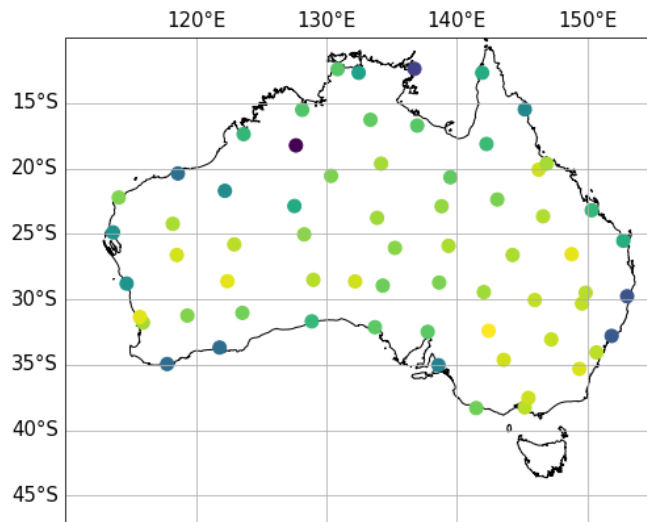
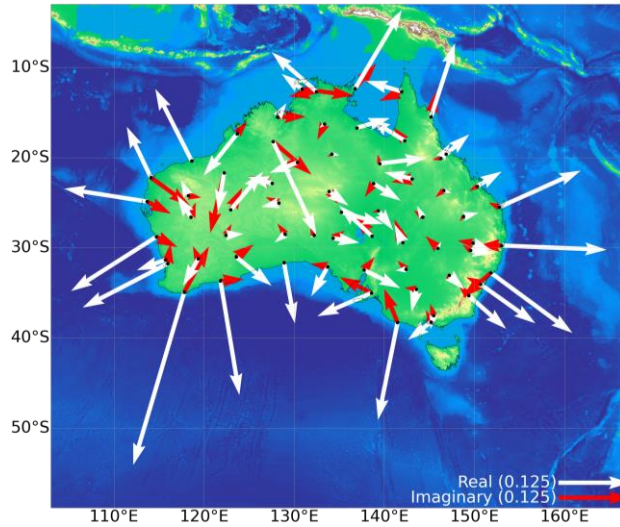
# Inversion of tippers from AWAGS data



Wang et al. 2014

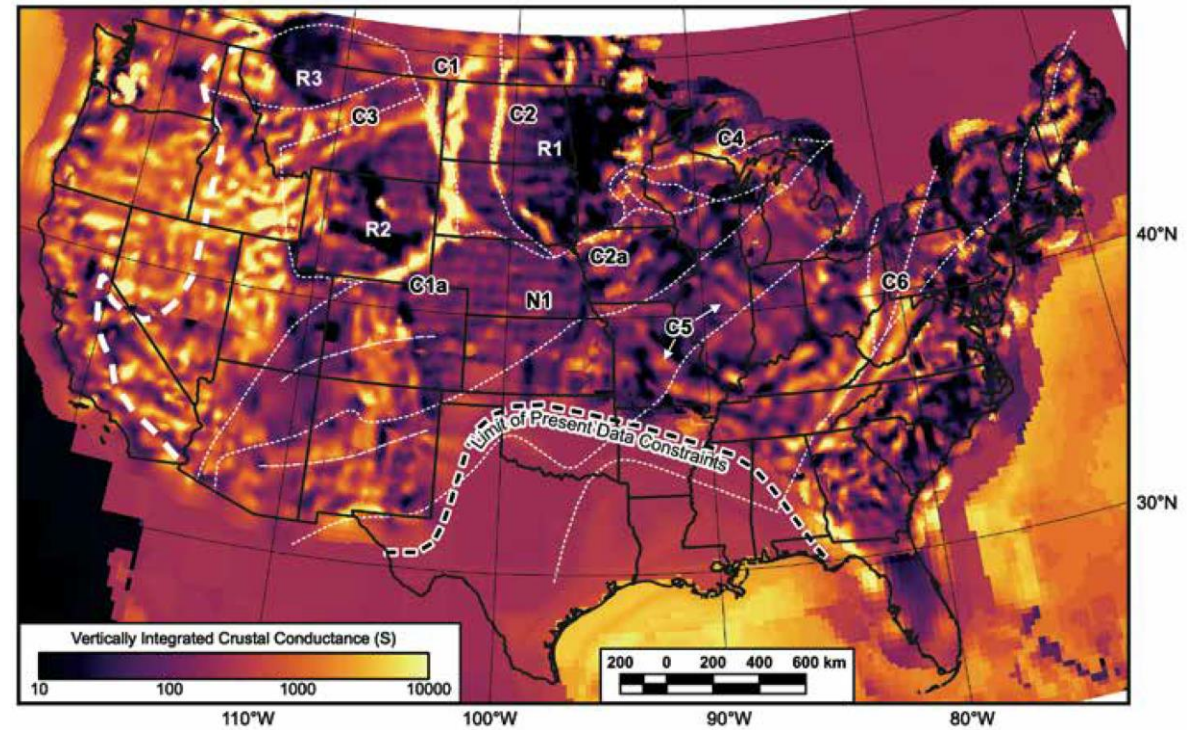
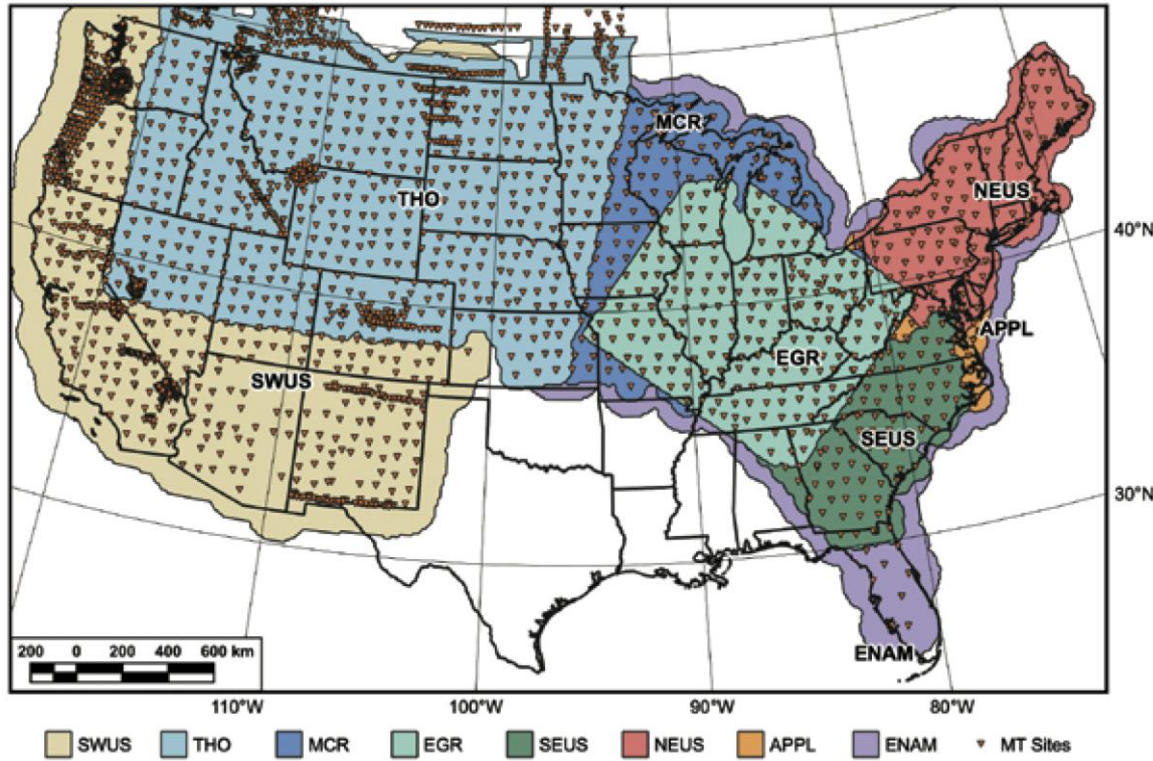
# Inversion of tippers from AWAGS data

Cicchetti, Grayver et al. 2022





# Inversion of USArray



Murphy et al. 2023; Kelbert et al. 2019

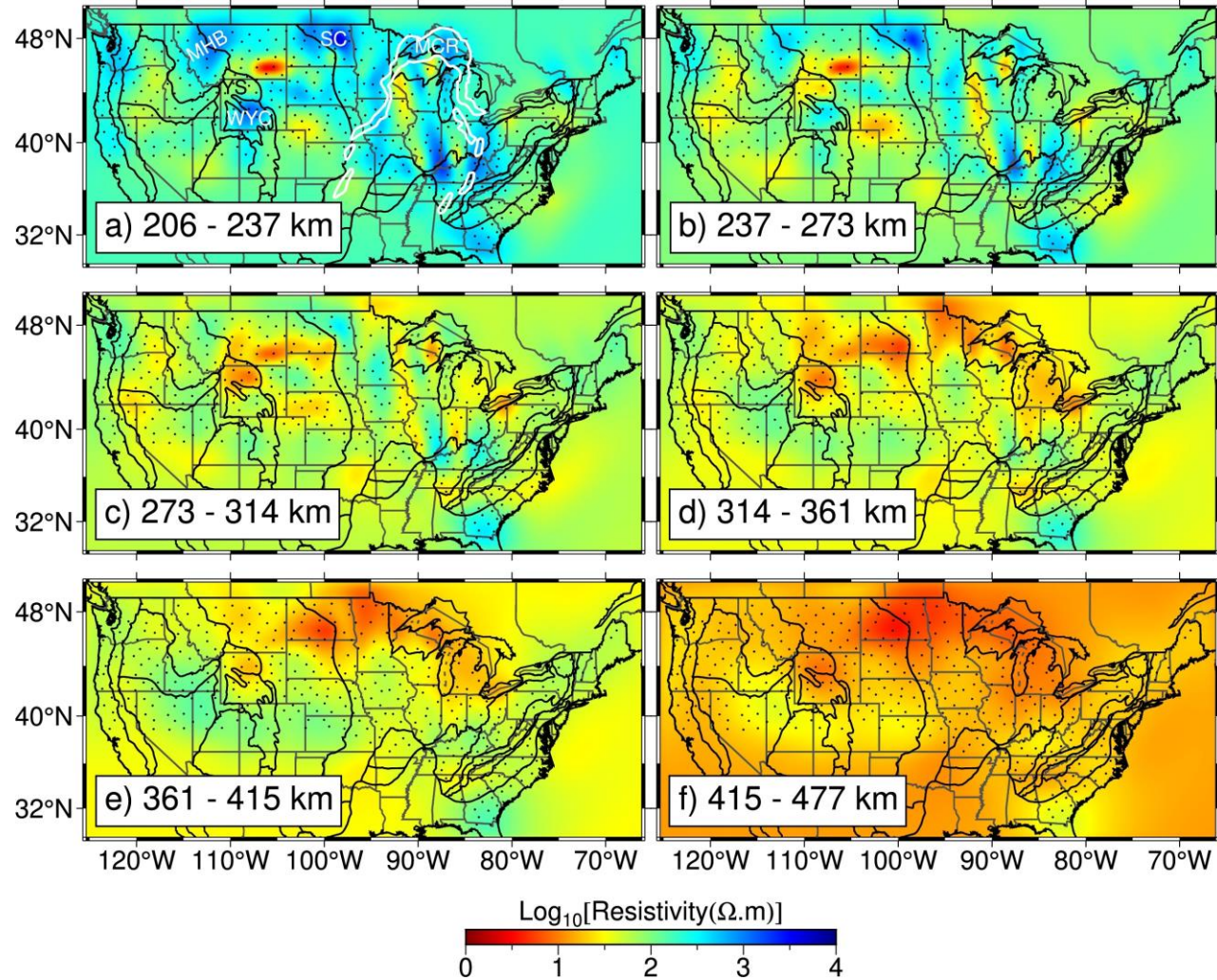
> 1500 stations in total, regional Cartesian models, merged posteriori



# Inversion of USArray

Yang and Egbert 2021

~500 stations, decimated array, Cartesian

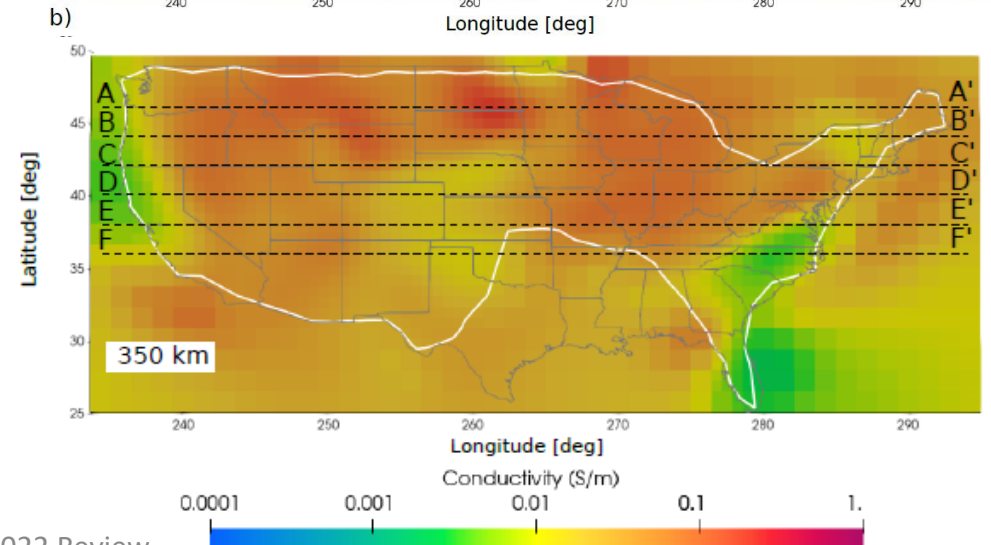
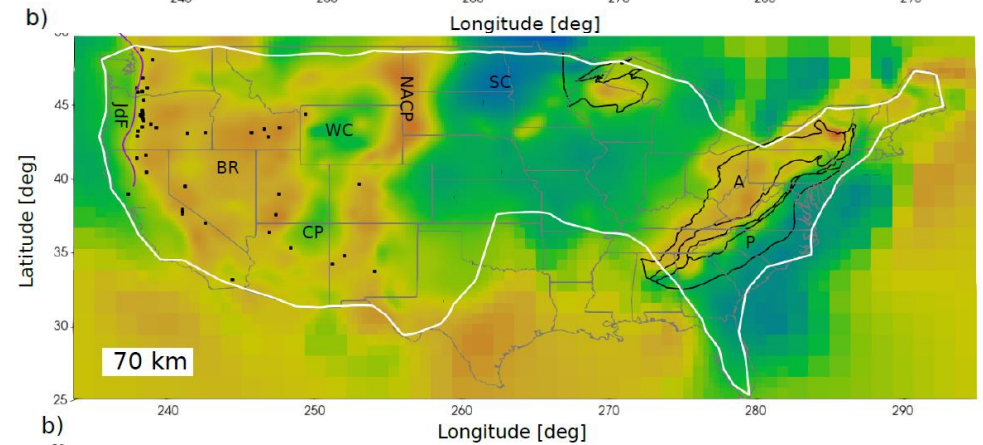
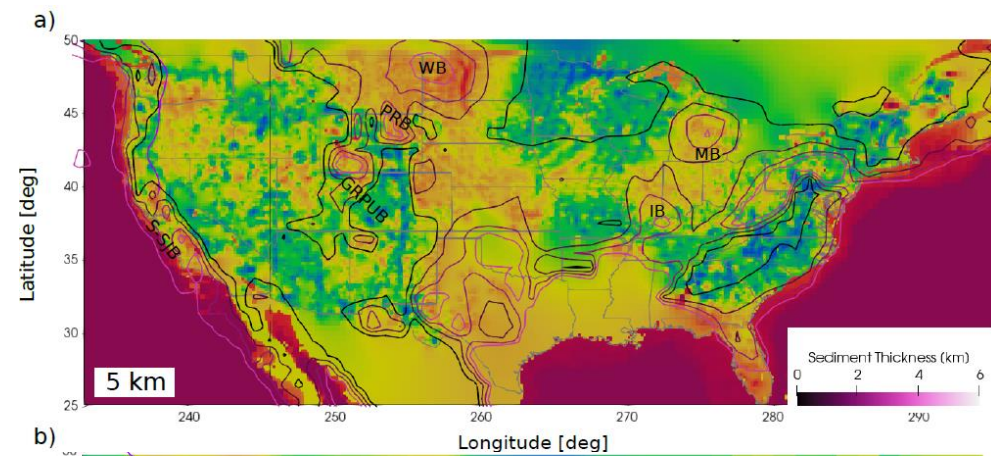
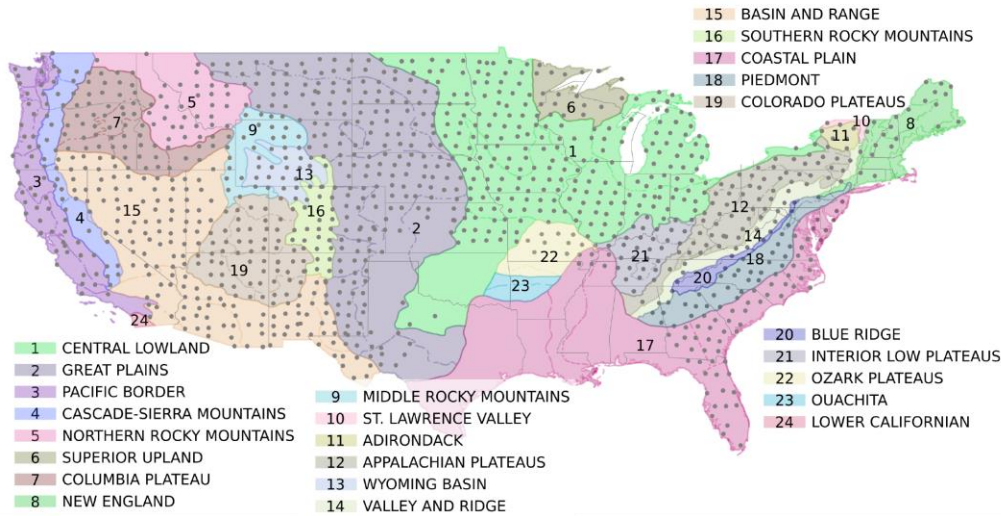




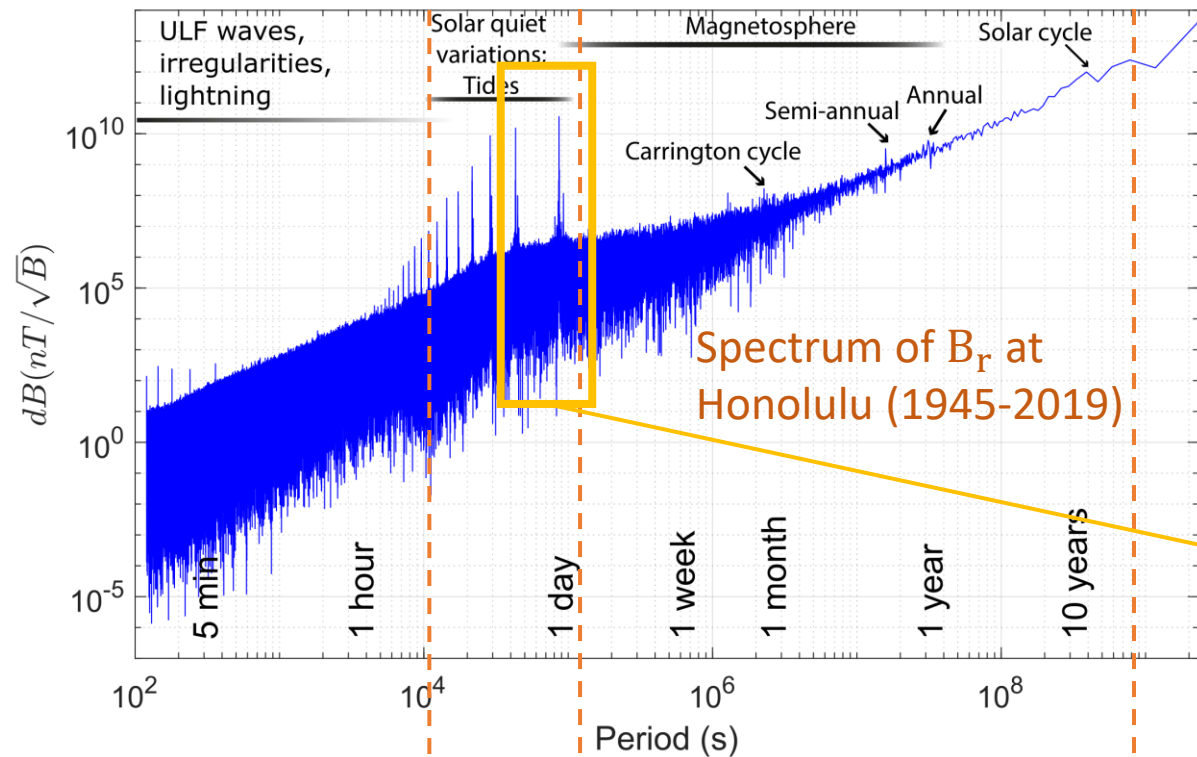
# Inversion of USArray

Munch and Grayver 2023, EPSL

1300 stations, nominal array resolution, Spherical

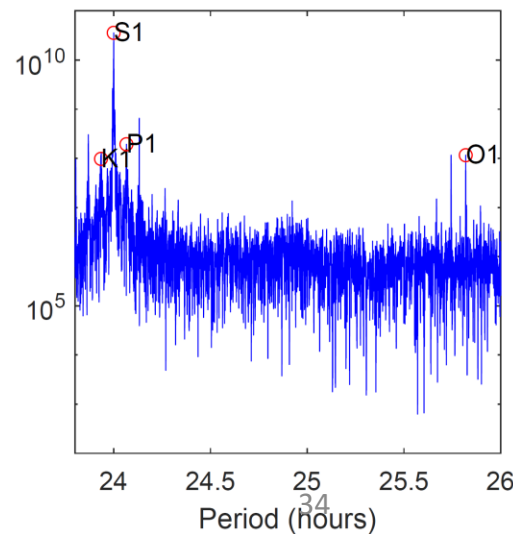
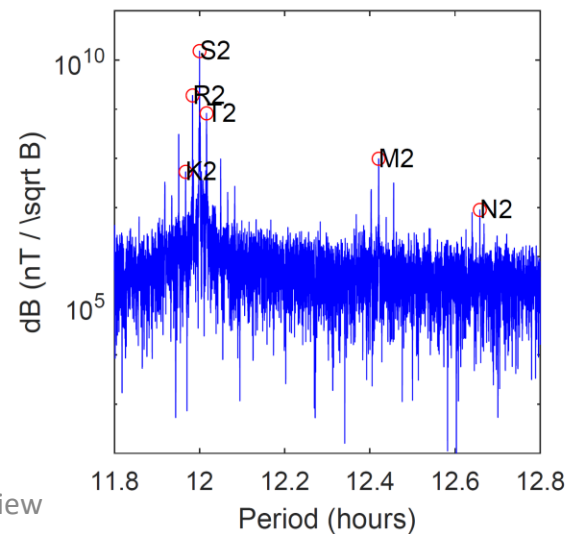


# Oceanic sources



Band: "Plane wave" "Daily" "Magnetospheric"

Sounding depth (km): < 350 200-500 > 400



# Oceanic sources: motivation

- Upper mantle below oceans is a key to understanding many geodynamic processes: MOR and subduction, plumes, etc...
- Marine MT is possible, but very expensive.
- Satellite-detected tidal magnetic signals appear the only source for global sounding of sub-oceanic mantle.

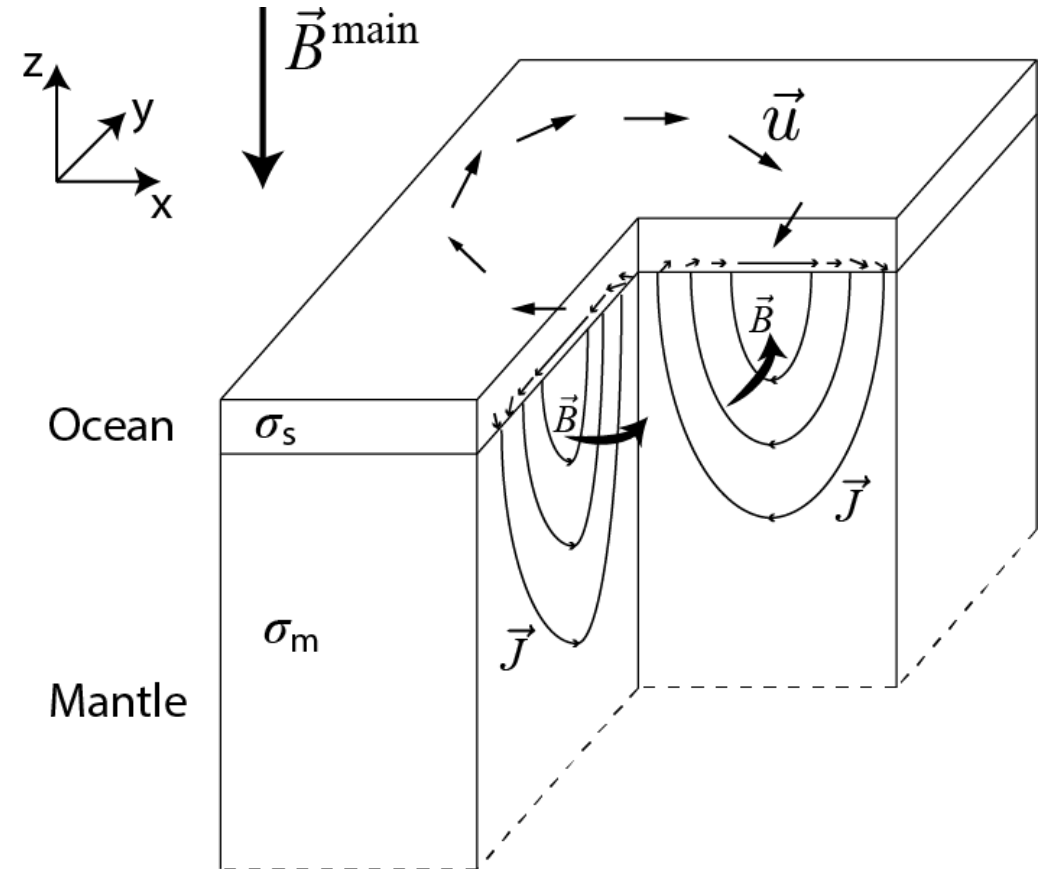
# Motional induction

- pre-Maxwell's equations (in frequency domain):

$$\begin{aligned}\nabla \times \vec{E} &= -i\omega\mu\vec{H} \\ \nabla \times \vec{H} &= \vec{j}\end{aligned}$$

- The current term consists of conduction and extraneous terms:

$$\vec{j} = \sigma\vec{E} + \underbrace{\sigma(\vec{u} \times \vec{B}^{main})}_{\text{current induced by the flow}}$$



*Reworked after Tyler 1997*

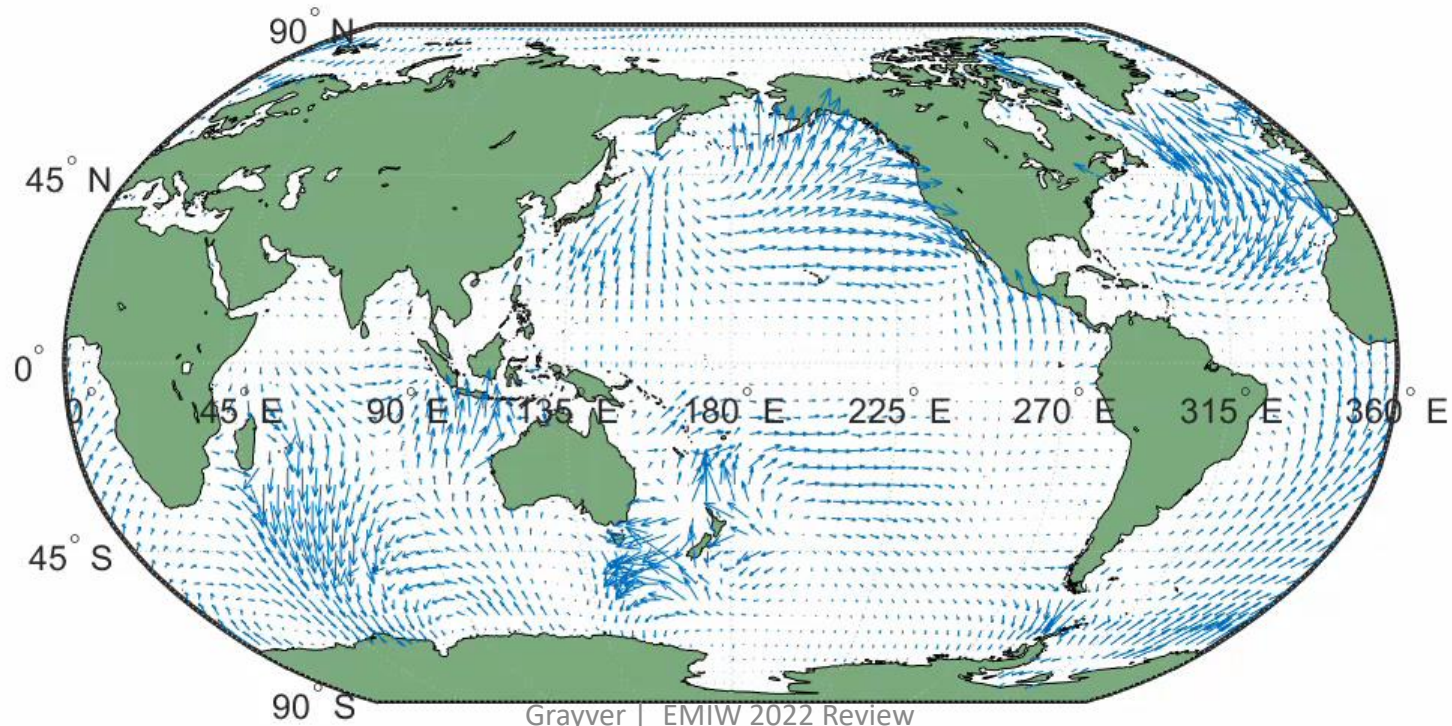


# Example: electric current due to M2 tide

- This animation shows electric currents induced by the M2 semi-diurnal lunar tide (as given by the TPXO model of G. Egbert) calculated as:

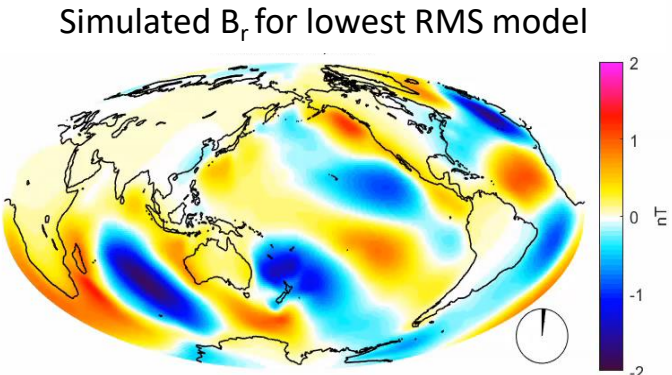
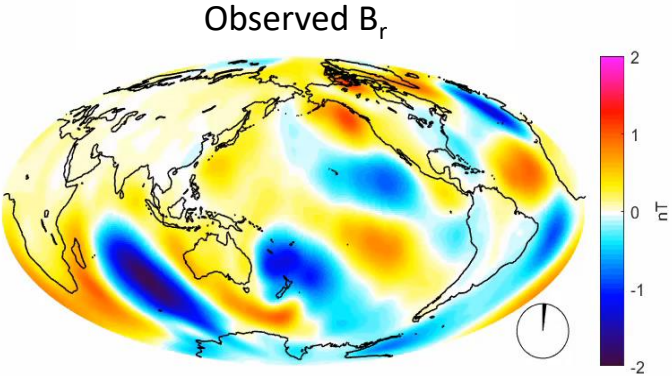
$$\vec{j}^{ext}(\vec{r}, \omega_{M2}) = \sigma_s(\vec{r}) \left[ \vec{u}_{M2}(\vec{r}, \omega_{M2}) \times \vec{B}^{main}(\vec{r}) \right]$$

Electric current due to semi-diurnal tide (12 hr 25 min). Time: 0.00 hours



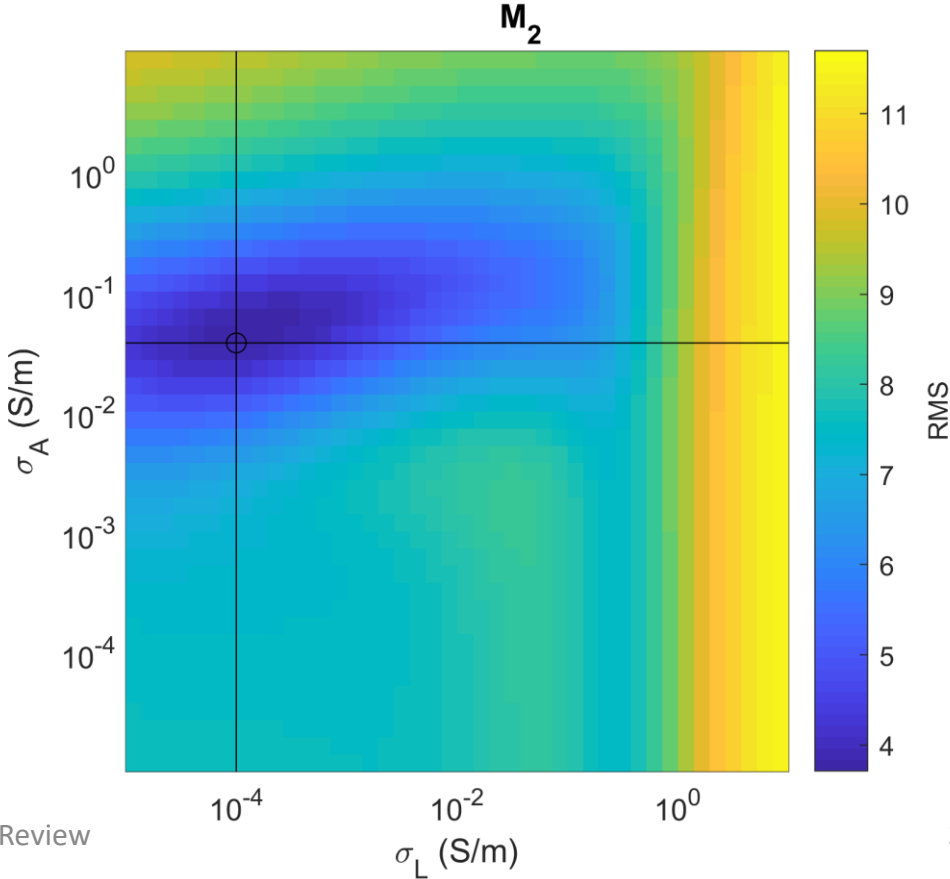
# Sounding upper mantle below the oceans with tides

- Principal lunar semidiurnal  $M_2$  (Period = 12.42 hours)



Grayver and Olsen, GRL, 2019

- Sensitivity to the conductivity of lithosphere ( $\sigma_L$ ) and asthenosphere ( $\sigma_A$ ) (LAB thickness is fixed to 70 km)



Grayver and Olsen 2019

# Use of tidal signals for conductivity imaging

## **Studies on mantle conductivity with tidal signals:**

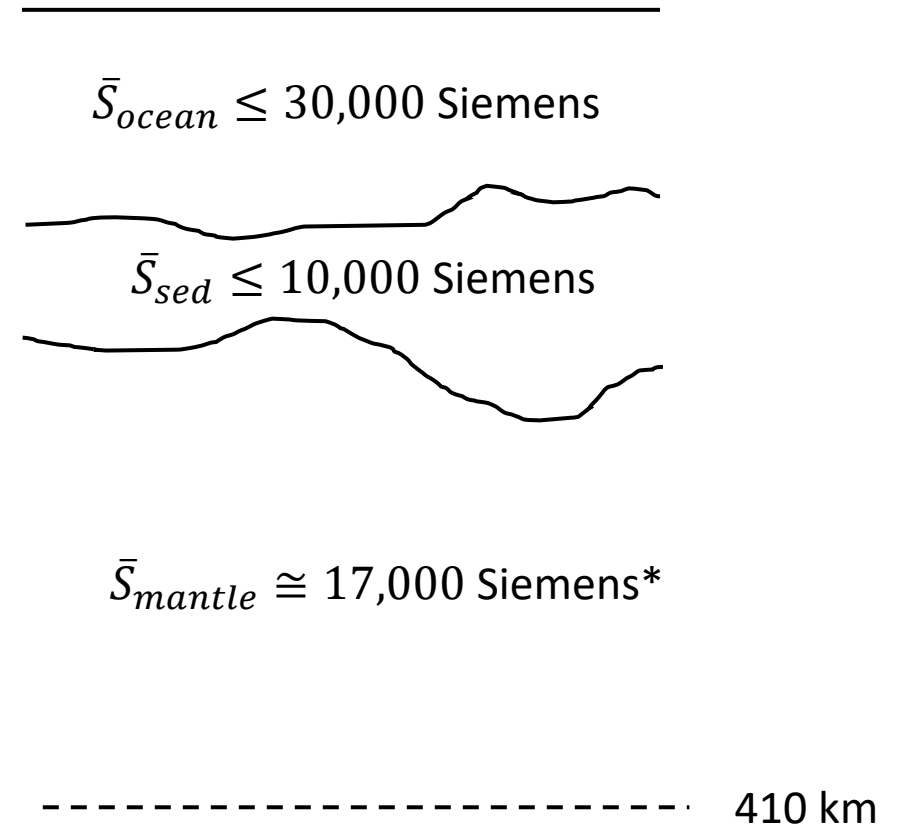
- Schnepf et al. 2015: sensitivity study to the upper mantle conductivity.
- Grayver et al. 2016: global ocean mantle conductivity profile from satellite M2 magnetic signals
- Grayver et al. 2017: Joint inversion of tidal and magnetospheric sources.
- Zhang et al. 2019: constraints on pacific LAB from observed seafloor tidal signals.
- Martinec et al. 2021: 3-D modelling study with real-data validation.
- Sachl et al. 2022: 3-D inversion of tidal magnetic signals (synthetic study).

## **Mapping global tidal signals:**

- Sabaka et al. 2015: mapped satellite magnetic signals due to the M2 tide globally (CI approach).
- Gayver and Olsen 2019: Extraction of M2, O1 and N2 constituents (sequential approach).
- Sabaka et al. 2020: M2, O1, N2 mapped (CI approach)
- Saynisch-Wagner et al. 2021: mapped several constituents using Kalman-filter approach

# Conductivity models of the ocean and sediments

- Average conductance of the ocean and marine sediments is equivalent to that of the entire upper mantle.
- Complex non-linear effect due to ocean and marine sediments in a wide range of periods.



# Conductivity models of the ocean and sediments

From Grayver 2021, G3

**Table 1**  
*Open Data Sets of Electrical Conductivity of the Ocean and Marine Sediments*

Source	Lateral resolution	Ocean conductivity	Sediment lateral resolution	Sediment conductivity
This study	0.1°–0.25°	3-D <sup>a</sup>	5 <sup>m</sup> <sup>b</sup>	3-D
Reagan et al. (2019)	0.25°	3-D <sup>c</sup>	N/A	N/A
Tyler et al. (2017)	1°	3-D <sup>d</sup>	N/A	N/A
Grayver et al. (2016)	1°	2-D <sup>e</sup>	N/A	N/A
Alekseev et al. (2015)	0.25°	Uniform $\sigma = 3.0$ S/m	1 <sup>of</sup>	0.5 S/m (water depth $\leq 500$ m) 0.7 S/m (water depth $> 500$ m)
Everett et al. (2003)	1°	Uniform $\sigma = 3.2$ S/m	1 <sup>of</sup>	0.8 S/m $\leq 7,000$ m.b.s.l. 0.02 S/m $> 7,000$ m.b.s.l. <sup>g</sup>

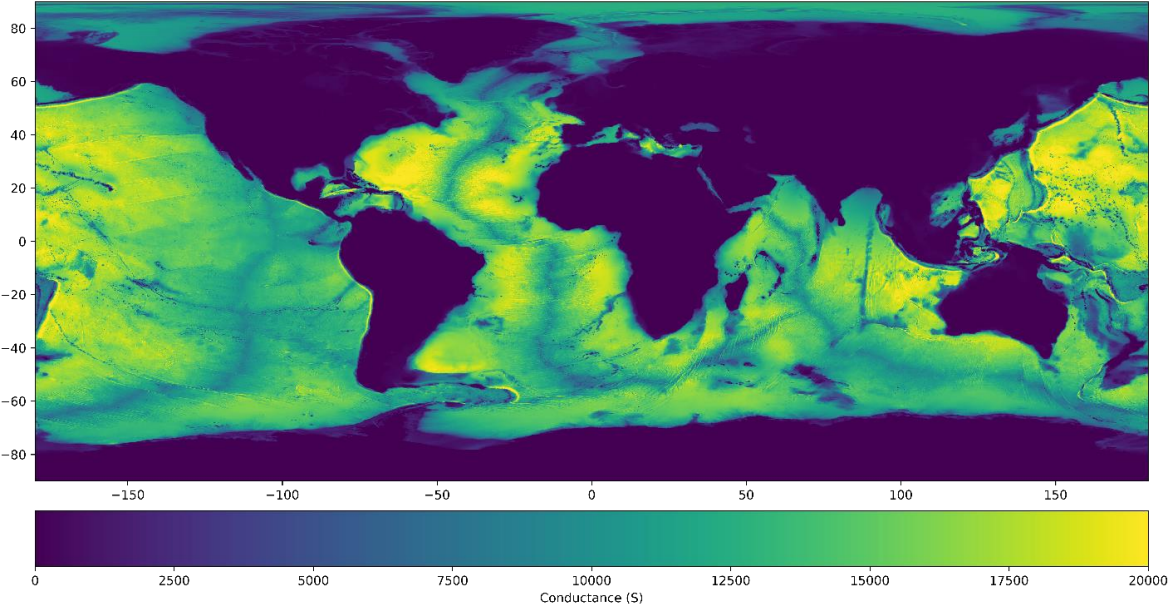
Note. “N/A” stands for not available.

<sup>a</sup>See Table 2 for more information on data sources. <sup>b</sup>GlodSed 5-arc-minute grid by Straume et al. (2019). <sup>c</sup>World Ocean Database 2018 (Boyer et al., 2013). <sup>d</sup>World Ocean Database 2013 (Boyer et al., 2013). <sup>e</sup>Depth-averaged conductivity based on World Ocean Atlas 2013 (Locarnini et al., 2013; Zweng et al., 2013). <sup>f</sup>Laske (1997). <sup>g</sup>“m.b.s.l.” stands for meters below sea level.

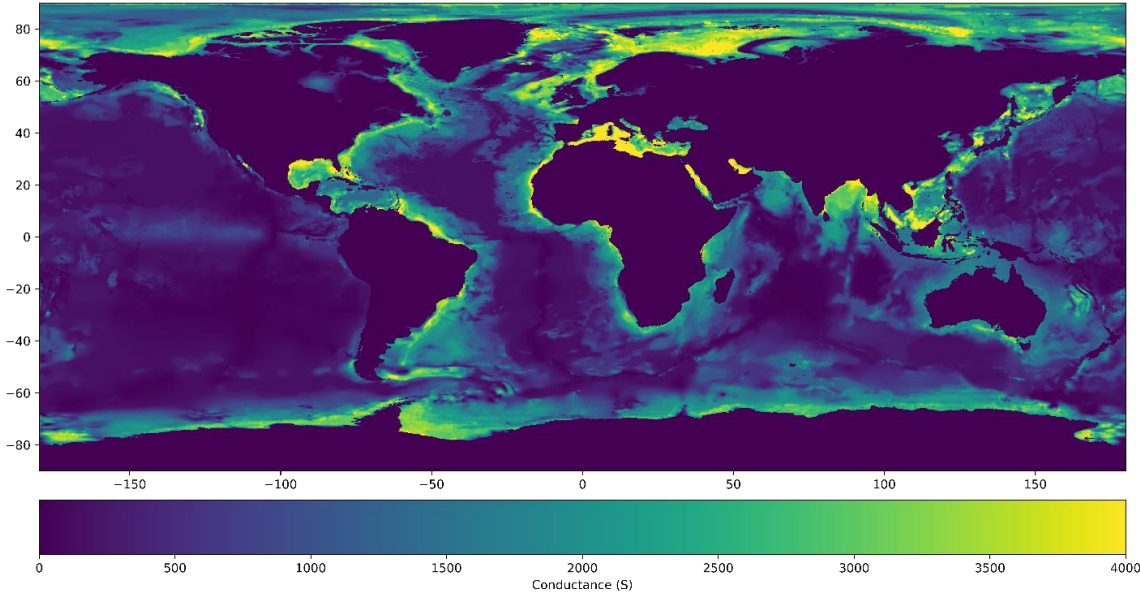


# Conductivity models of the ocean and sediments

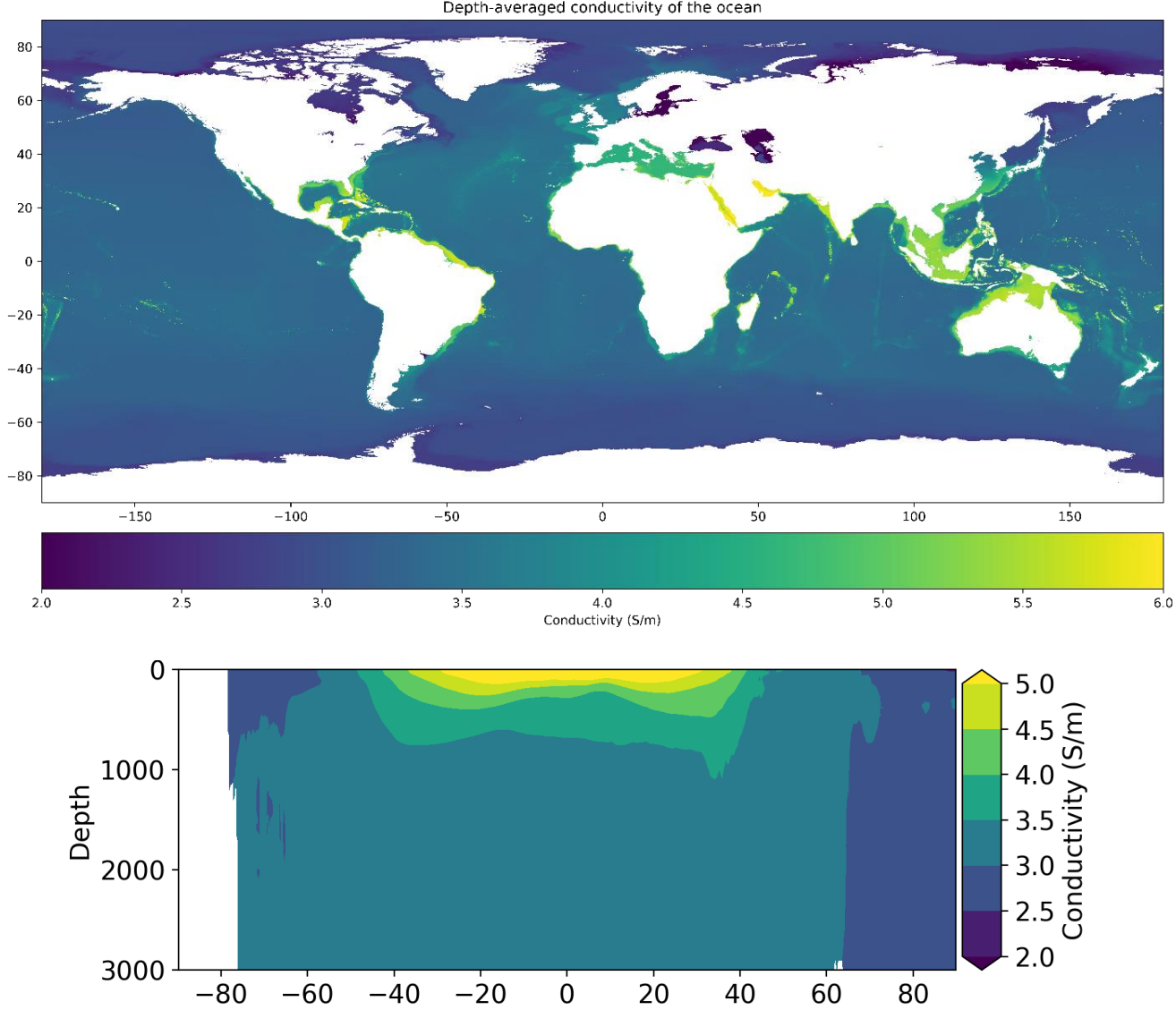
Ocean conductance



Marine sediments conductance



# Conductivity models of the ocean and sediments



# Handling complex (unknown) sources

# Magnetic field representation and GDS responses

Above the ground and in the source-free region,

$$\nabla \times \vec{B} = 0.$$

Therefore,  $\vec{B}$  is a potential field and can be written as

$$\vec{B} = -\nabla V. \quad (15)$$

By virtue of Gauss' law of magnetism,  $\nabla \cdot \vec{B} = 0$ . Thus, a scalar potential  $V$  satisfies the Laplace's equation,

$$\nabla^2 V = 0. \quad (16)$$



# Magnetic field representation and GDS responses

allow us to write the magnetic field above the Earth as

$$\vec{B}(\vec{r}, \omega) = \vec{B}(\vec{r}, \omega)^{\text{ext}} + \vec{B}(\vec{r}, \omega; \sigma)^{\text{int}}$$

or in the component form

$$\begin{aligned} B_r &= - \sum_{n,m} n \varepsilon_n^m(\omega) \left(\frac{r}{a}\right)^{n-1} S_n^m(\theta, \phi) \\ &\quad + \sum_{k,l} (k+1) \iota_k^l(\omega; \sigma) \left(\frac{a}{r}\right)^{k+2} S_k^l(\theta, \phi), \\ \vec{B}_\tau &= - \sum_{n,m} \varepsilon_n^m(\omega) \left(\frac{r}{a}\right)^{n-1} \nabla_\perp S_n^m(\theta, \phi) \\ &\quad - \sum_{k,l} \iota_k^l(\omega; \sigma) \left(\frac{a}{r}\right)^{k+2} \nabla_\perp S_k^l(\theta, \phi), \end{aligned}$$

Where:

$$\sum_{n,m} = \sum_{n=1}^{\infty} \sum_{m=-n}^n$$

$$S_n^m(\theta, \phi) = P_n^{|m|}(\cos \theta) \exp(im\phi)$$

# Magnetic field representation and GDS responses

Magnetic field within a conductive body (slightly below the surface, assuming 1-D radial conductivity):

$$B_r(\vec{r}_a, \omega; \sigma) = \sum_{n,m} (2n+1)n\epsilon_n^m(\omega) \frac{Z_n}{i\omega\mu_0 a - nZ_n} S_n^m(\theta, \phi), \quad (1)$$

$$\vec{B}_\tau(\vec{r}_a, \omega; \sigma) = - \sum_{n,m} \frac{2n+1}{n+1} \epsilon_n^m(\omega) \frac{i\omega\mu_0 a}{i\omega\mu_0 a - nZ_n} \nabla_\perp S_n^m(\theta, \phi). \quad (2)$$

Here,  $Z_n \equiv Z_n(r, \omega; \sigma)$  is the spectral impedance of a spherical conductor (e.g. Srivastava 1966).

**Assuming** that the external inducing field is described by a **single** spherical harmonic  $S_n^m$  and noting that  $Z_n = -i\omega\mu_0 C_n$ , the local  $C_n$  response becomes:

$$C_n = \frac{a}{n(n+1)} \frac{\partial_\theta S_n^m}{S_n^m} \frac{B_r}{B_\theta}.$$

**If** the geometry of the inducing field is described by the first zonal harmonic  $S_1^0 = P_1^0$ , we get

$$C_1 = -\frac{a}{2} \tan \theta \frac{B_r}{B_\theta},$$

← Z/H method (Banks 1969), GDS response

# What is the problem with Z/H method?

If the geometry of the inducing field is described by the **single** first zonal harmonic  $S_1^0 = P_1^0$ , we get

$$C_1 = -\frac{a}{2} \tan \theta \frac{B_r}{B_\theta},$$

← Z/H method (Banks 1969), GDS response

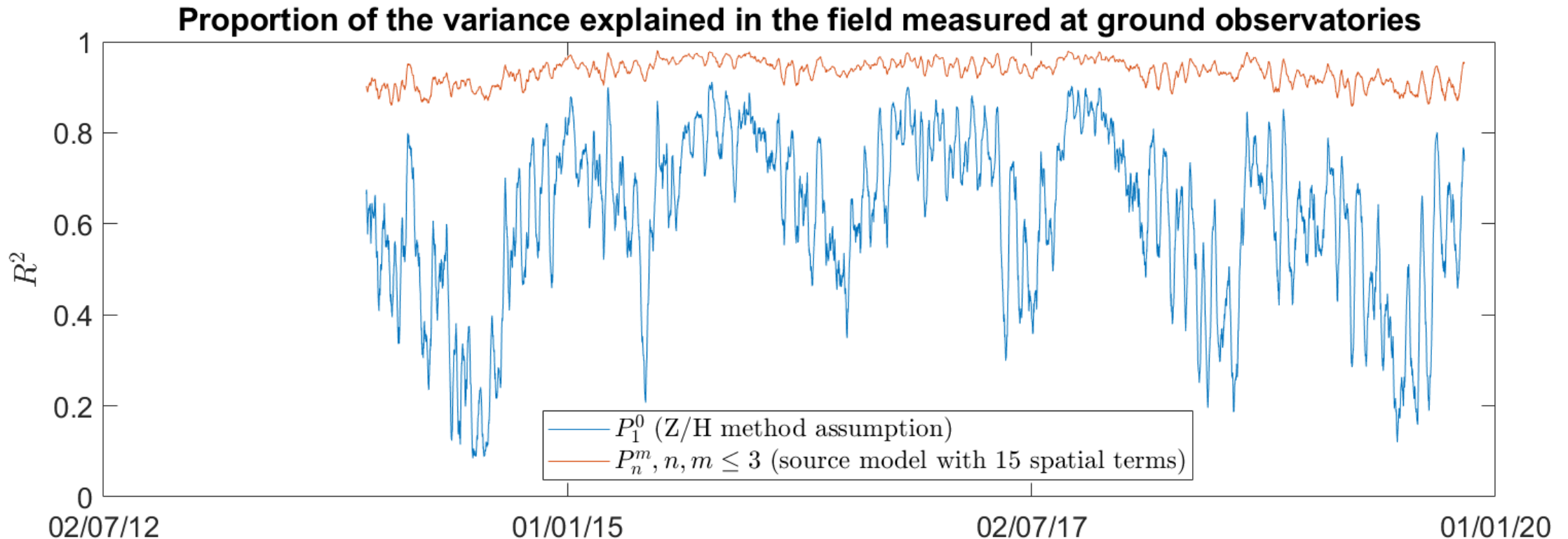
- Source is always more complex than P10, even at mid geomagnetic latitudes.
- Assuming P10 still ok for global average 1-D models → source effects are averaged.
- Not ok for global/regional 3-D studies because:
  - Inverse problem is highly non-unique due to sparse data
  - Source effects are much stronger than 3-D response from deep mantle anomalies
  - Source effects propagate to the conductivity model in an uncontrolled way
  - Impossible to discriminate between source effects and 3-D conductivity

# What is the problem with Z/H method?

If the geometry of the inducing field is described by the **single** first zonal harmonic  $S_1^0 = P_1^0$ , we get

$$C_1 = -\frac{a}{2} \tan \theta \frac{B_r}{B_\theta},$$

← Z/H method (Banks 1969), GDS response



\*Only mid geomagnetic latitude observatories ( $5^\circ$ - $56^\circ$ ) are used.



# What is the problem with Z/H method?

If the geometry of the inducing field is described by the **single** first zonal harmonic  $S_1^0 = P_1^0$ , we get

$$C_1 = -\frac{a}{2} \tan \theta \frac{B_r}{B_\theta},$$

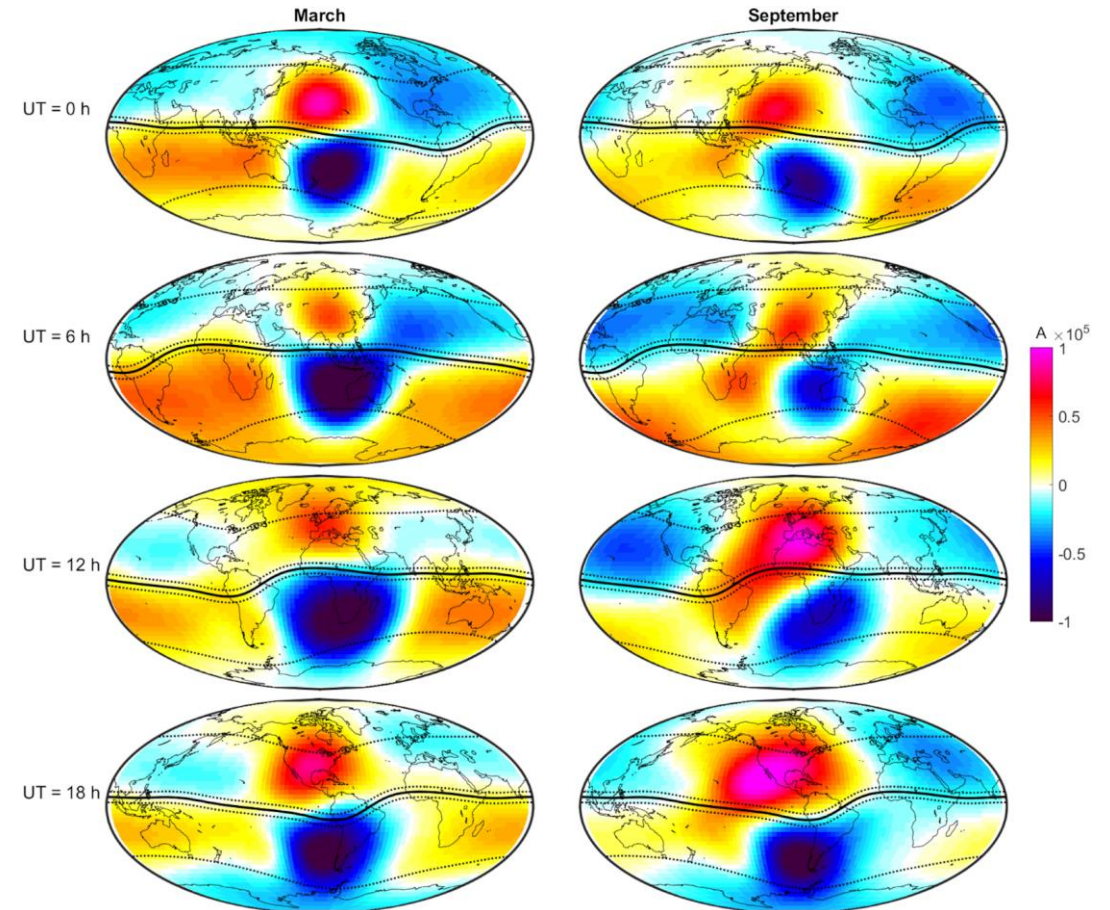
← Z/H method by Banks (1969), GDS response

- Source is always more complex than P10, even at mid geomagnetic latitudes.
- Assuming P10 still ok for global average 1-D models → source effects are averaged.
- Not ok for global/regional 3-D studies because:
  - Inverse problem is highly non-unique due to sparse data
  - Source effects are much stronger than 3-D response from deep mantle anomalies
  - Source effects propagate to the conductivity model in an uncontrolled way
  - Impossible to discriminate between source effects and 3-D conductivity
- **Solution?** Acknowledge the source is complicated and invest into methods that can handle complex and more realistic sources.

# Handling complex sources

- Spatial parameterization:
  - General basis using spherical harmonics (Olsen 1999, Schmucker 1999, Pütke and Kuvshinov 2014, Guzavina et al. 2019)
  - Physics-based basis (Egbert et al. 2021; Zenhausern et al. 2021)
  - Current loops representation (Martinec et al. 2022)

Sq current system for a magnetically quiet day

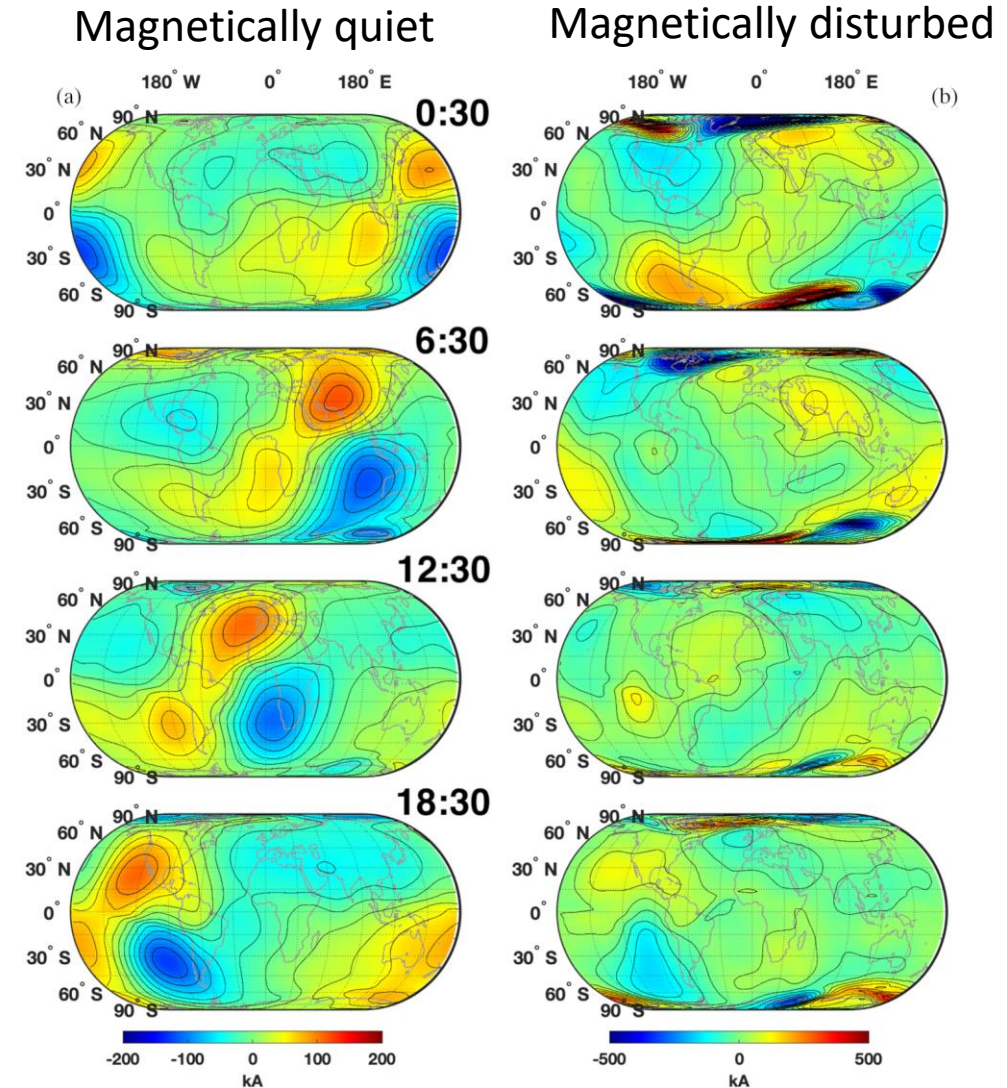


Guzavina et al. 2019

# Handling complex sources

- Spatial parameterization:
  - General basis using spherical harmonics (Olsen 1999, Schmucker 1999, Pütke and Kuvshinov 2014, Guzavina et al. 2019)
  - Physics-based basis (Egbert et al. 2021; Zenhausern et al. 2021)
  - Current loops representation (Martinec et al. 2022)

## Equivalent current system



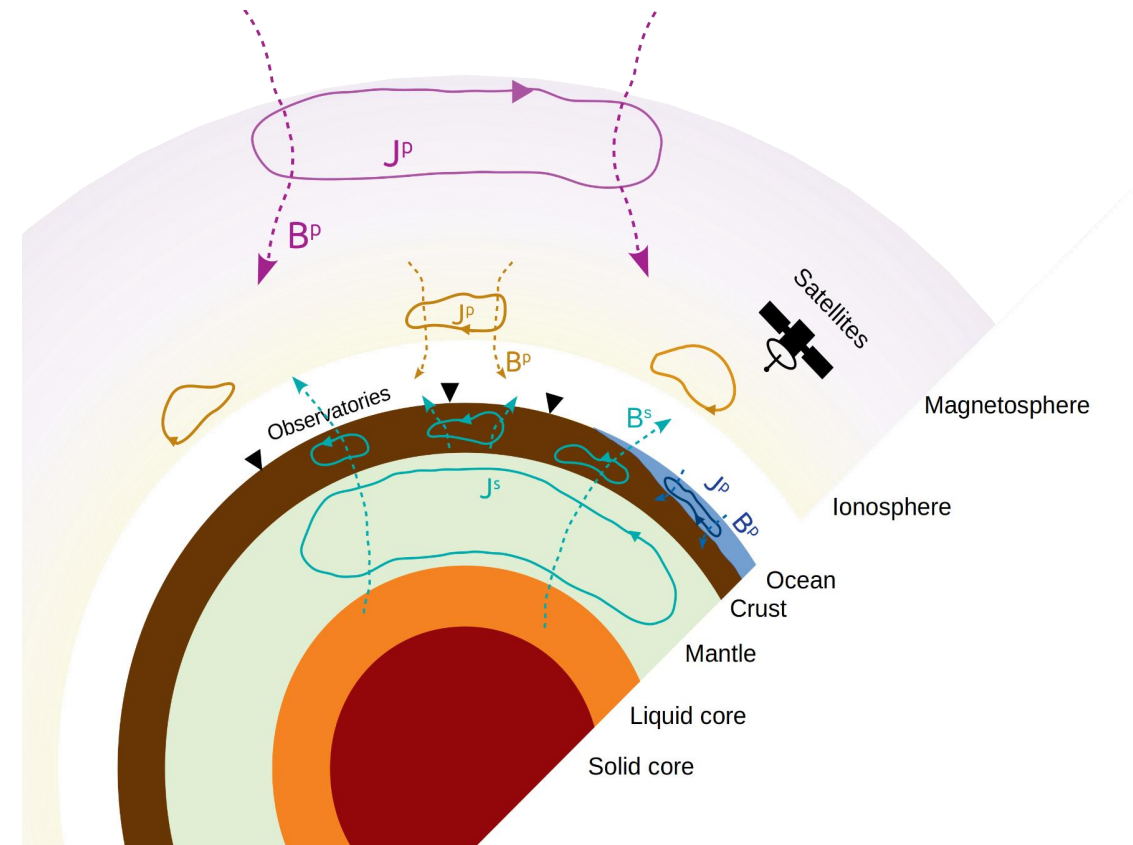
Egbert et al. 2021

# Handling complex sources

Separable non-linear least squares (SNLS):

$$(1) \min_{\sigma, j^p} \|d - F(\sigma)j^p\|_2^2 + R(\sigma, j^p)$$

How to solve a SNLS problem?





# Solving SNLS problem: Alternating approach

Separable non-linear least squares (SNLS):

$$(1) \min_{\sigma, j^p} \|d - F(\sigma)j^p\|_2^2 + R(\sigma, j^p)$$

How to solve a SNLS problem?

- 1) Assume a fixed  $\sigma_0$ , then eq. (1) becomes a linear problem for  $j^p$
- 2) Solve linear problem for source estimate  $\tilde{j}^p$
- 3) Use source estimate  $\tilde{j}^p$  to solve a non-linear problem for  $\tilde{\sigma}$ .
- 4) Go to step (1) and use new  $\tilde{\sigma}$

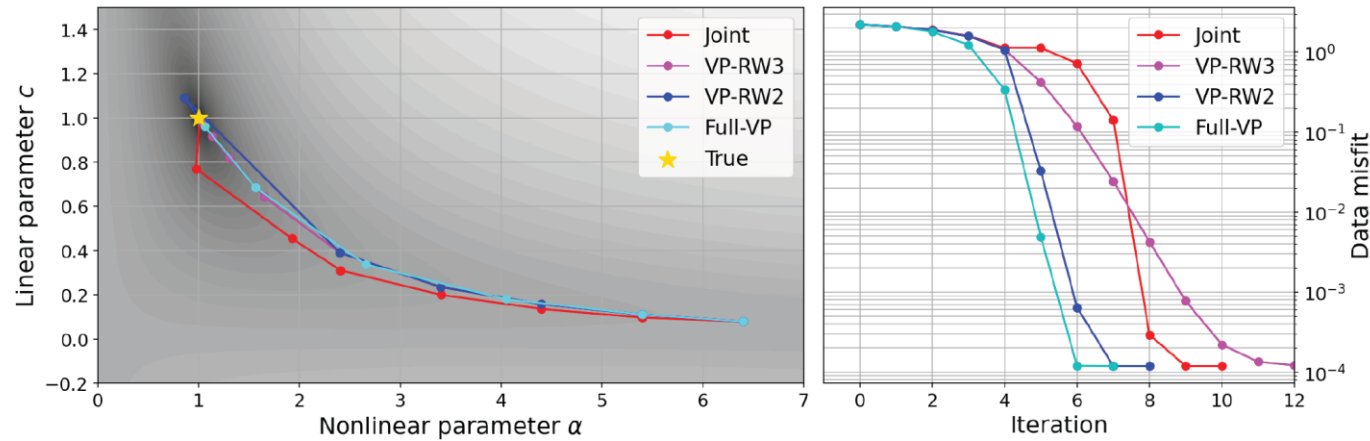


# Solving SNLS problem: Alternating approach

- Koch and Kuvshinov 2013: ionospheric Sq signals, regional 3-D inversion
- Pütke et al. 2015: generalization to arbitrary sources, 3-D
- Guzavina et al. 2019, Munch et al. 2020: inversion of ionospheric Sq + magnetospheric signals
- Zhang et al. 2022: Sq inversion, physics-based parameterization
- Grayver et al. 2021: formulation in time domain, incorporation of satellites

# Solving SNLS problem: Variable Projection

$$\phi(t) = -\frac{d^2}{dt^2} (ce^{-\alpha t^2}) = 2c(\alpha - 2\alpha^2 t^2)e^{-\alpha t^2}$$

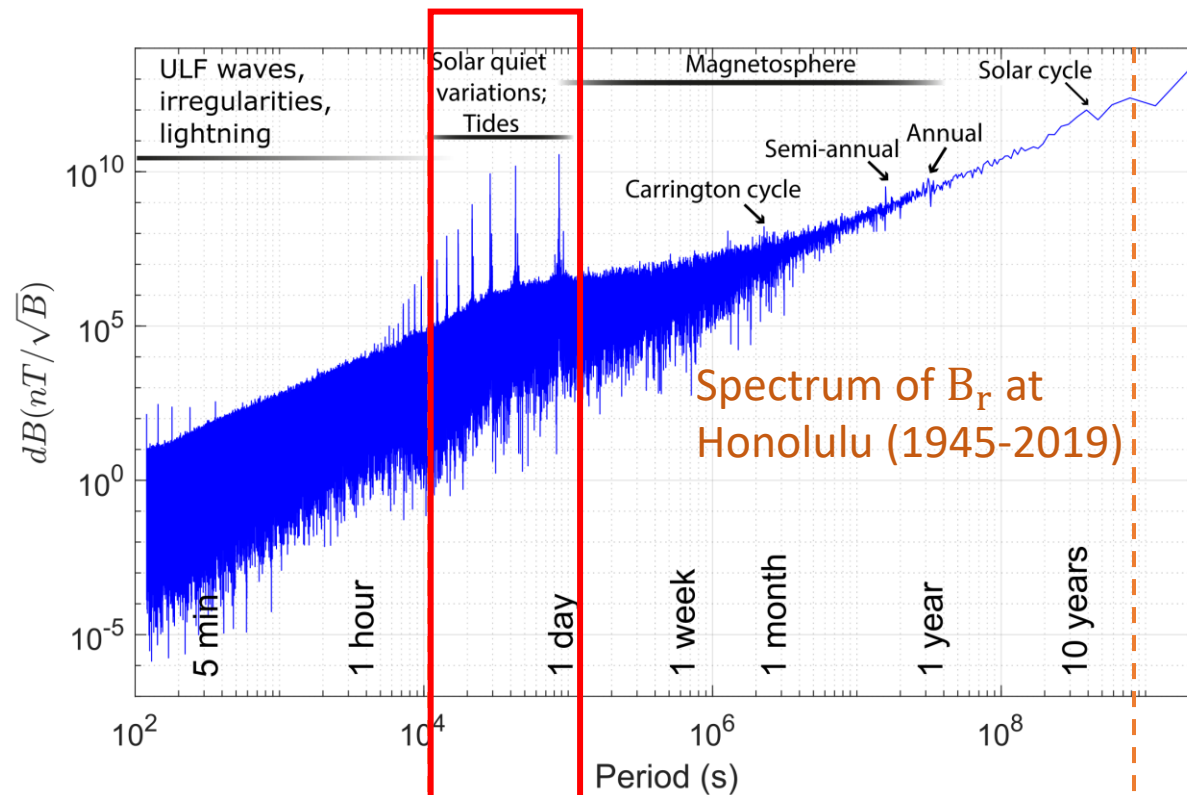


Variable Projection is the most efficient and consistent way to solve SNLS problems

Figure B.1. Convergence of different inversion techniques on the wavelet fitting problem. Left: trajectories of inversion schemes in the parameter space for the wavelet fitting problem. The background color shows the data misfit in logarithmic scale. Right: data misfit as a function of iteration.

Min, J. and Grayver A., 2023, “*Simultaneous inversion for source field and mantle electrical conductivity using the Variable Projection approach*”, Earth, Planets and Space, **accepted**

# Ionospheric sources: case studies



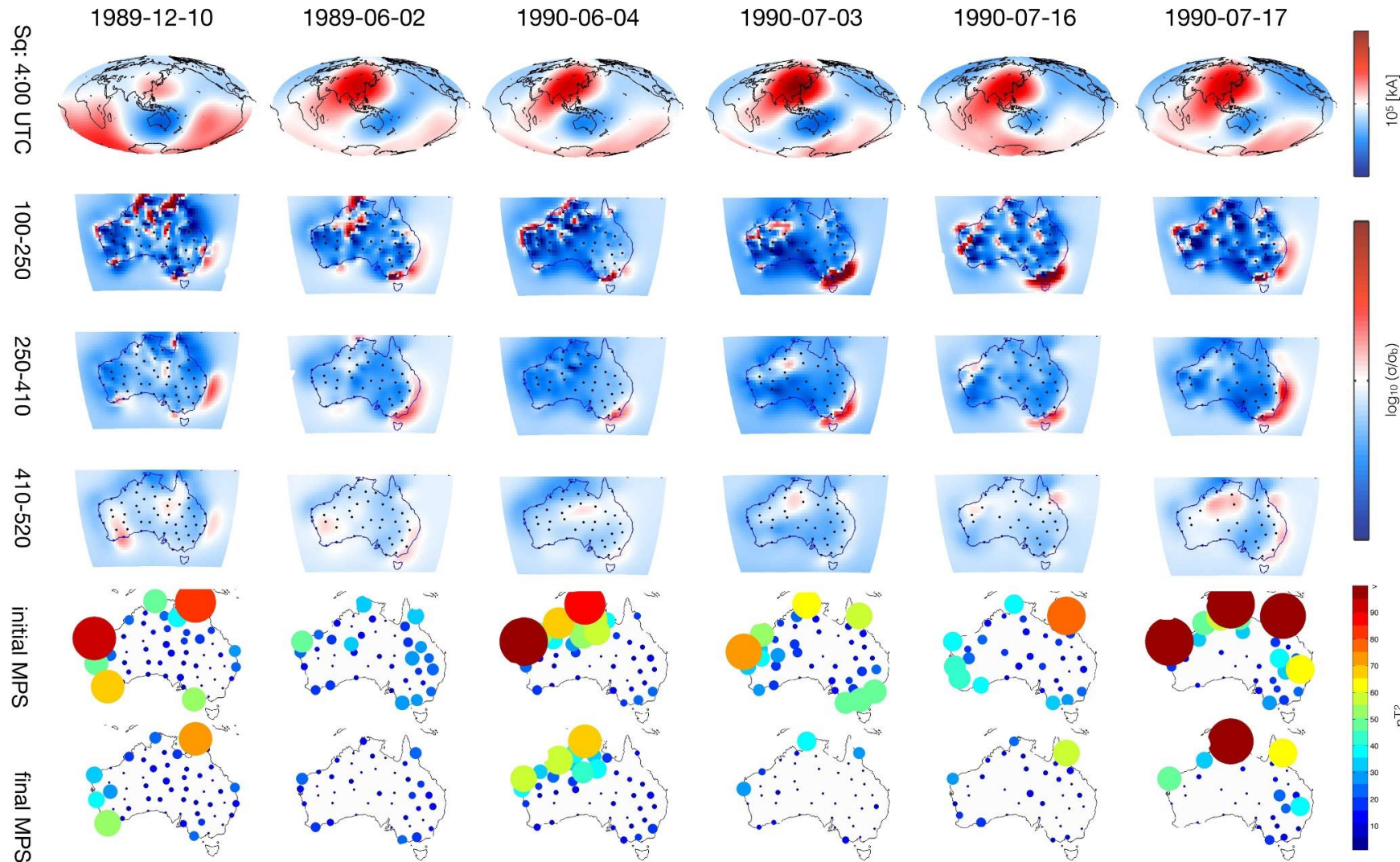
Spectrum of  $B_r$  at Honolulu (1945-2019)

Band: "Plane wave" "Daily" "Magnetospheric"

Sounding depth (km): < 350 200-500 > 400

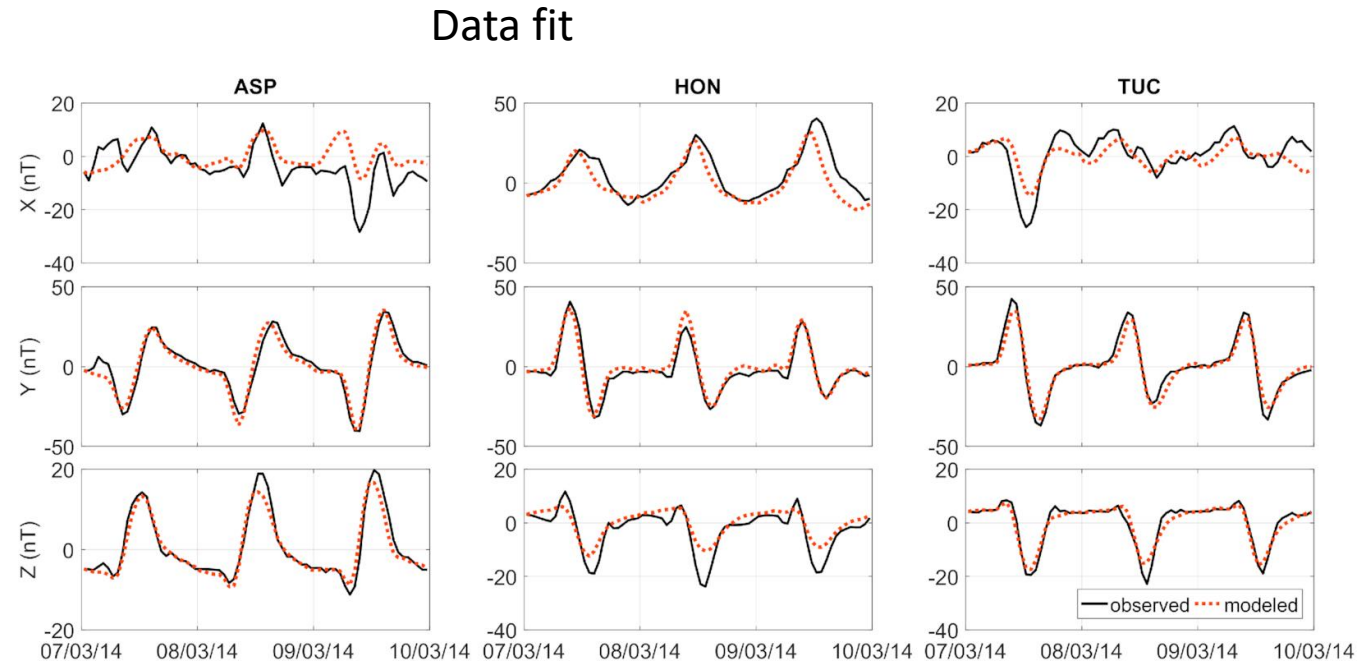
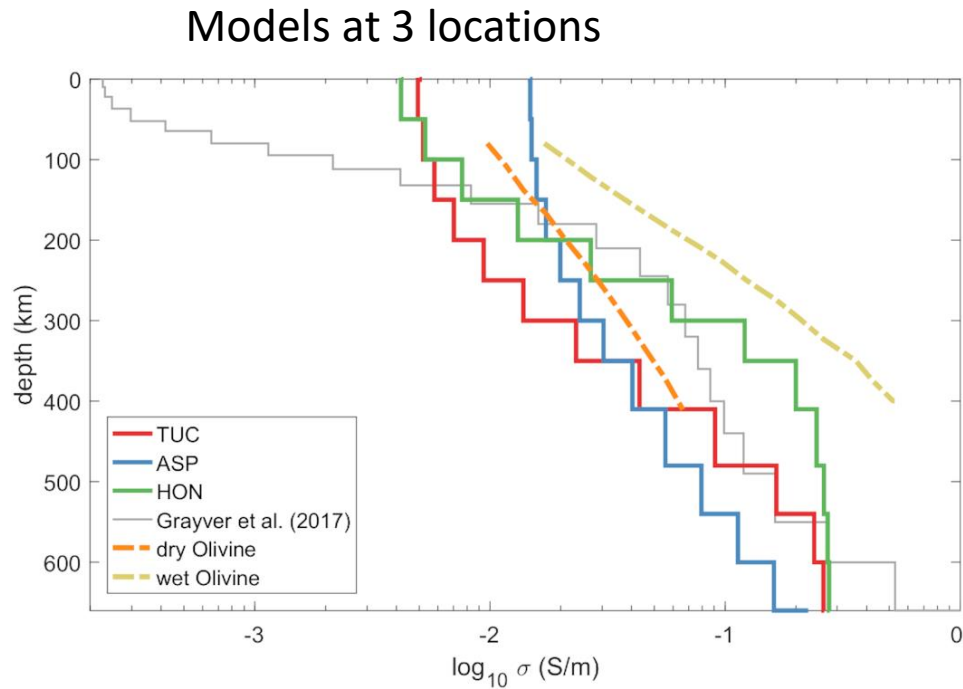


# Inversion of daily variations



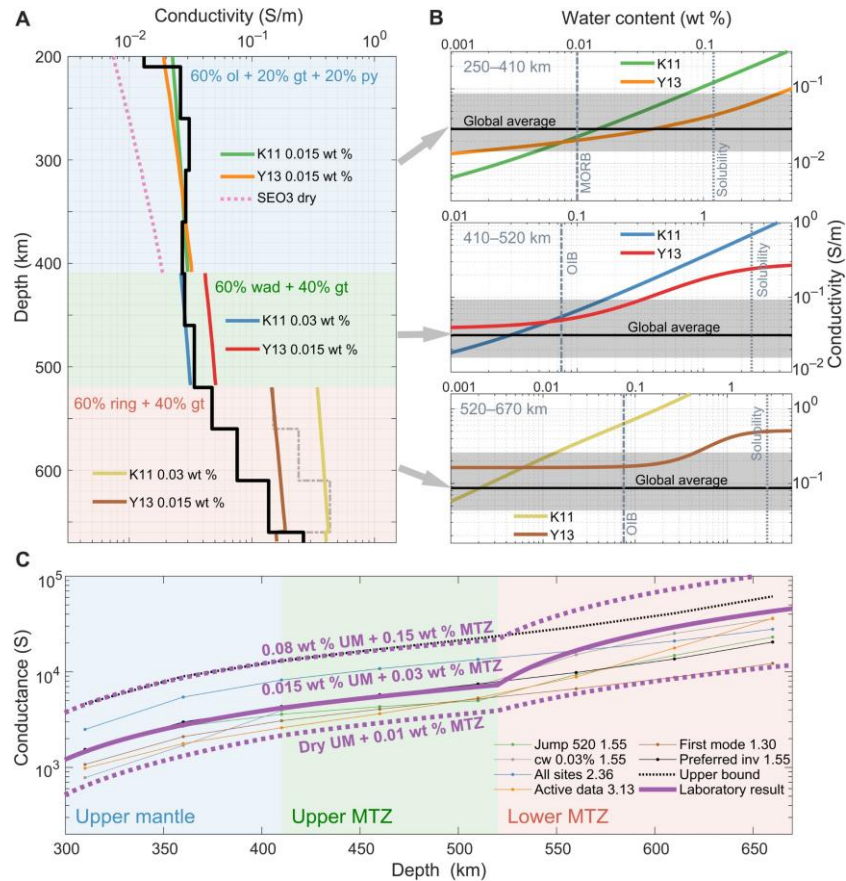
Koch and Kuvshinov 2015

# Inversion of daily variations



Guzavina et al. 2019

# Inversion of daily variations



Zhang et al. 2022, Egbert et al. 2021

Abstract, 25<sup>th</sup> EM Induction Workshop, Çeşme, Turkey, September 11-17, 2022

## Deep geomagnetic sounding by Sq variations in Europe: A 3-D inversion based on the regional-to-local transfer functions

J. Velínský<sup>1</sup>, L. Šachl<sup>1</sup> and O. Knopp<sup>1</sup>

<sup>1</sup>Dept. of Geophysics, Faculty of Mathematics and Physics, Charles University, Prague, Czech Republic, jakub.velimsky@mff.cuni.cz

Abstract, 25<sup>th</sup> EM Induction Workshop, Çeşme, Turkey, September 11-17, 2022

## Regionality of mantle conductivity inferred from geomagnetic daily variation analysis

Takao Koyama<sup>1</sup>, Shigeru Fujita<sup>2</sup>, Ikuko Fujii<sup>3</sup>, Kiyoshi Baba<sup>4</sup> and Hisayoshi Shimizu<sup>5</sup>

<sup>1</sup>Earthquake Research Institute, The University of Tokyo, tkoyama@eri.u-tokyo.ac.jp

<sup>2</sup>The Institute of Statistical Mathematics, sfujita@ism.ac.jp

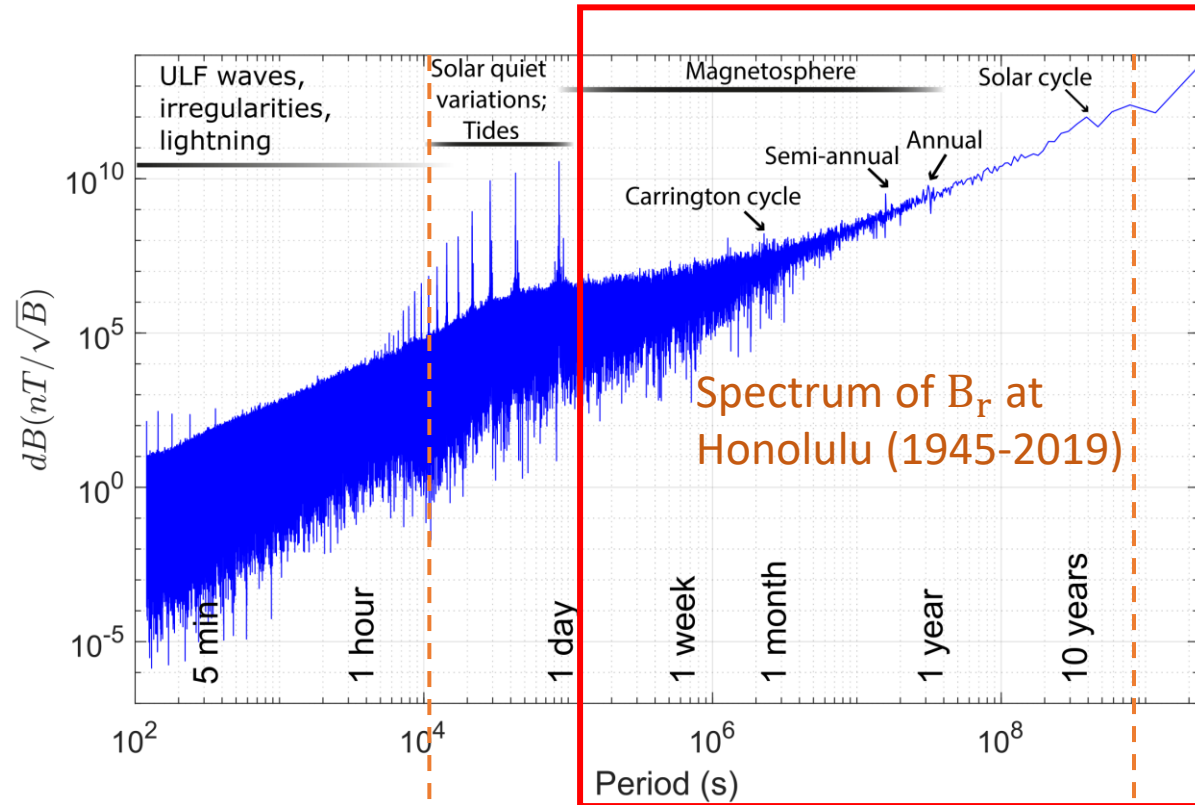
<sup>3</sup>Meteorological College, Japan Meteorological Agency, ifujii@mc-jma.go.jp

<sup>4</sup>Earthquake Research Institute, The University of Tokyo, kbaba@eri.u-tokyo.ac.jp

<sup>5</sup>Earthquake Research Institute, The University of Tokyo, shimizu@eri.u-tokyo.ac.jp

# Magnetospheric sources



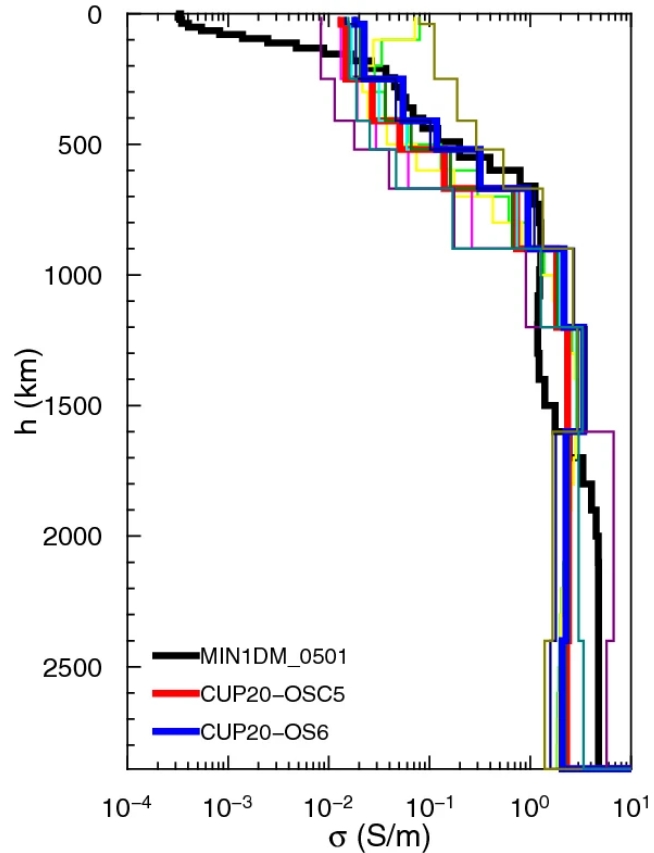


Band: "Plane wave" "Daily" "Magnetospheric"

Sounding depth (km): < 350 200-500 > 400

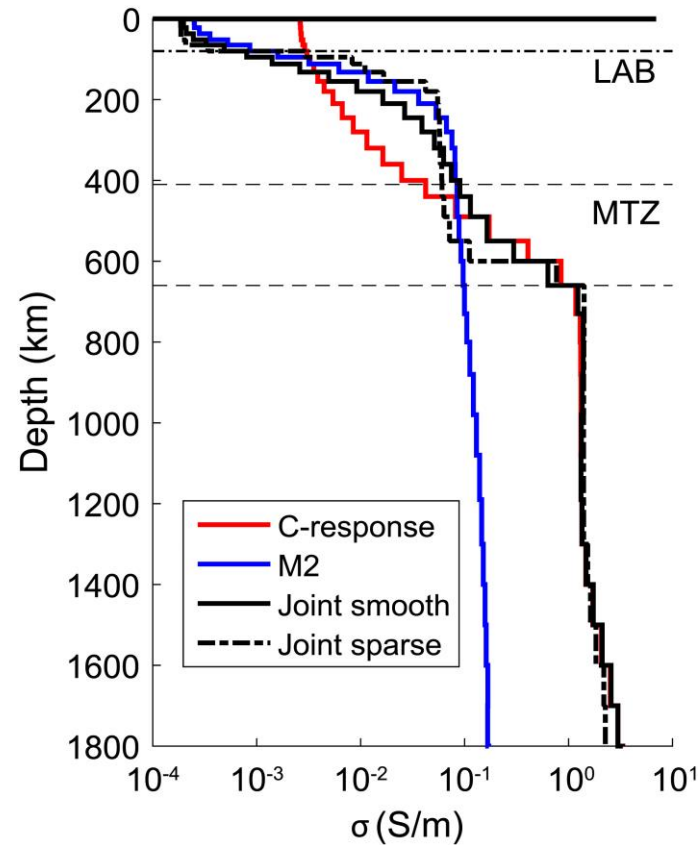
# Global average conductivity profiles: examples

Obs+Swarm,  
Ring current variations



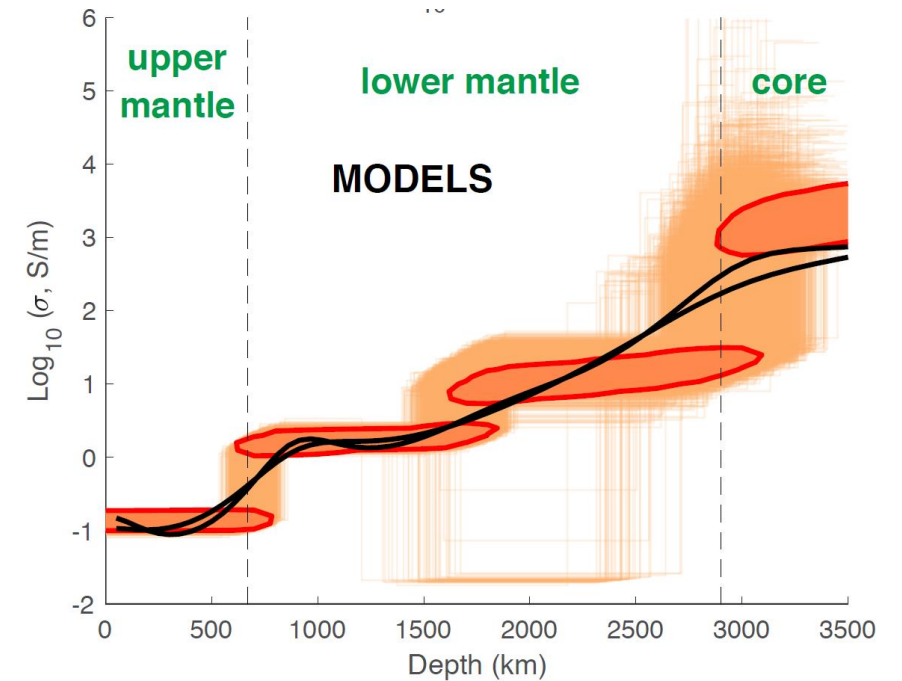
Velimsky et al. 2021

CHAMP+Swarm,  
Ring current + Tides



Grayver et al. 2017

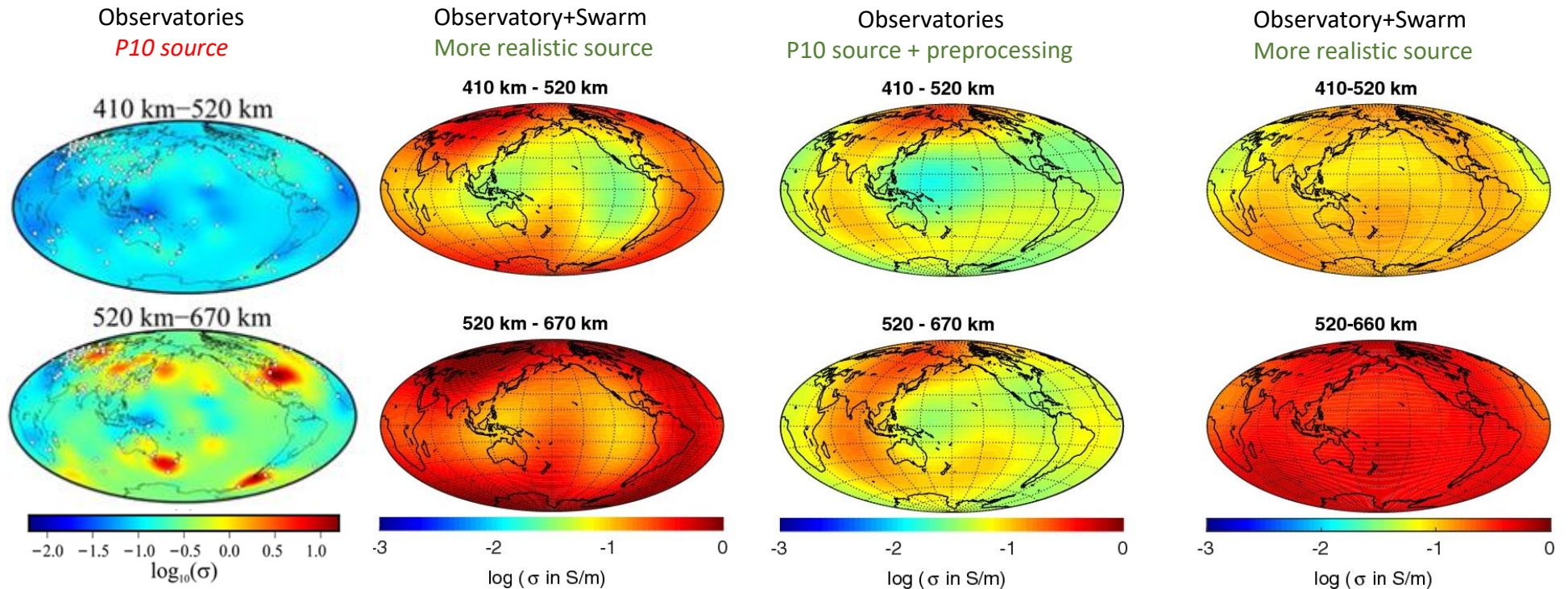
Observatories (> 100 years of data)  
Ring current variations (T up to 11 years)



Constable et al., in prep

# Present status of global 3-D models

- Resolution is still very low
- Insufficient data coverage



Li et al. 2021

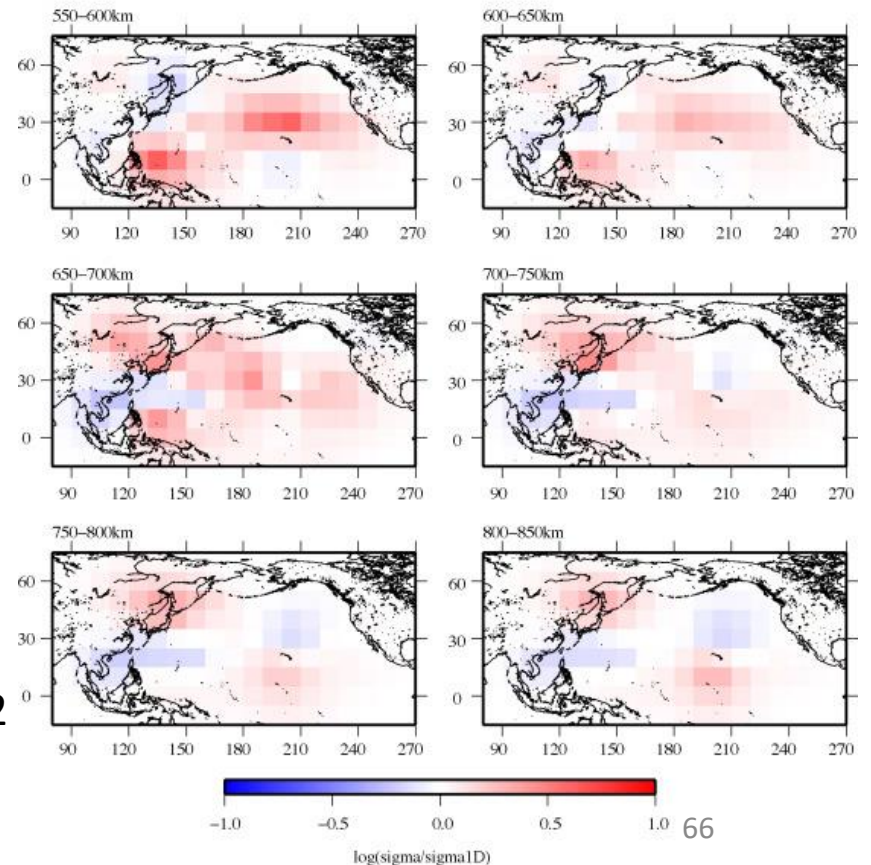
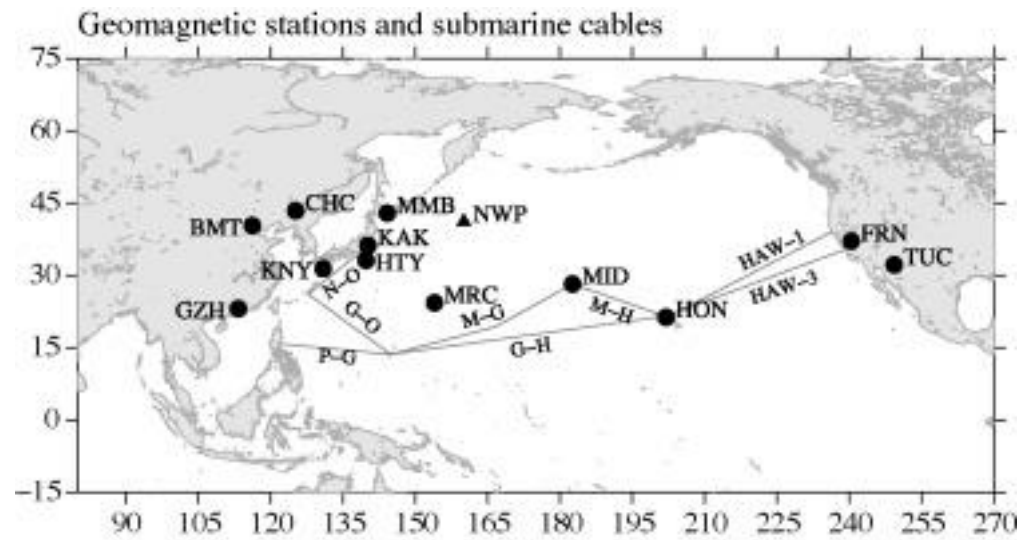
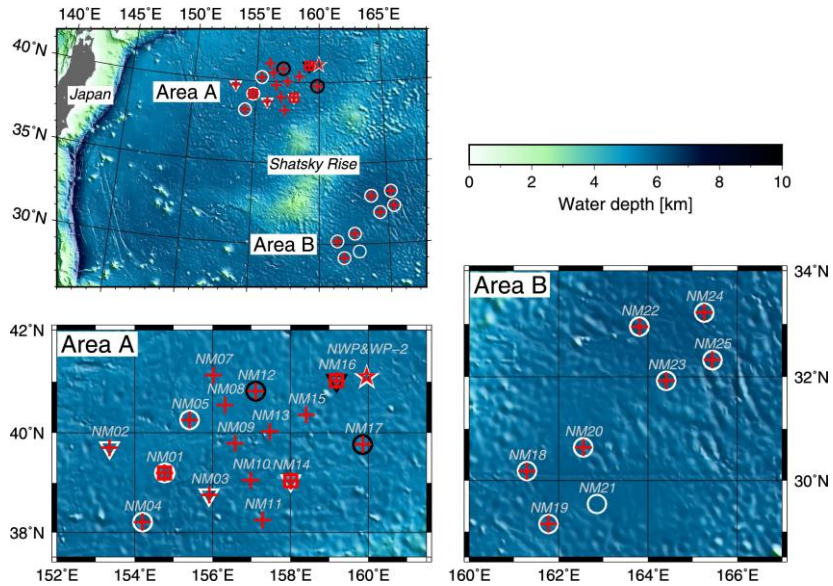
Velimsky et al. 2021

Kelbert et al. 2015

Kuvshinov et al. 2021

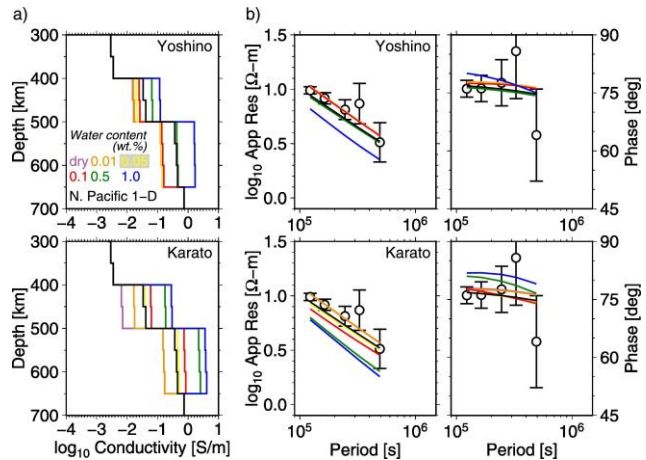


# Semi-global studies



*P10 source assumption*

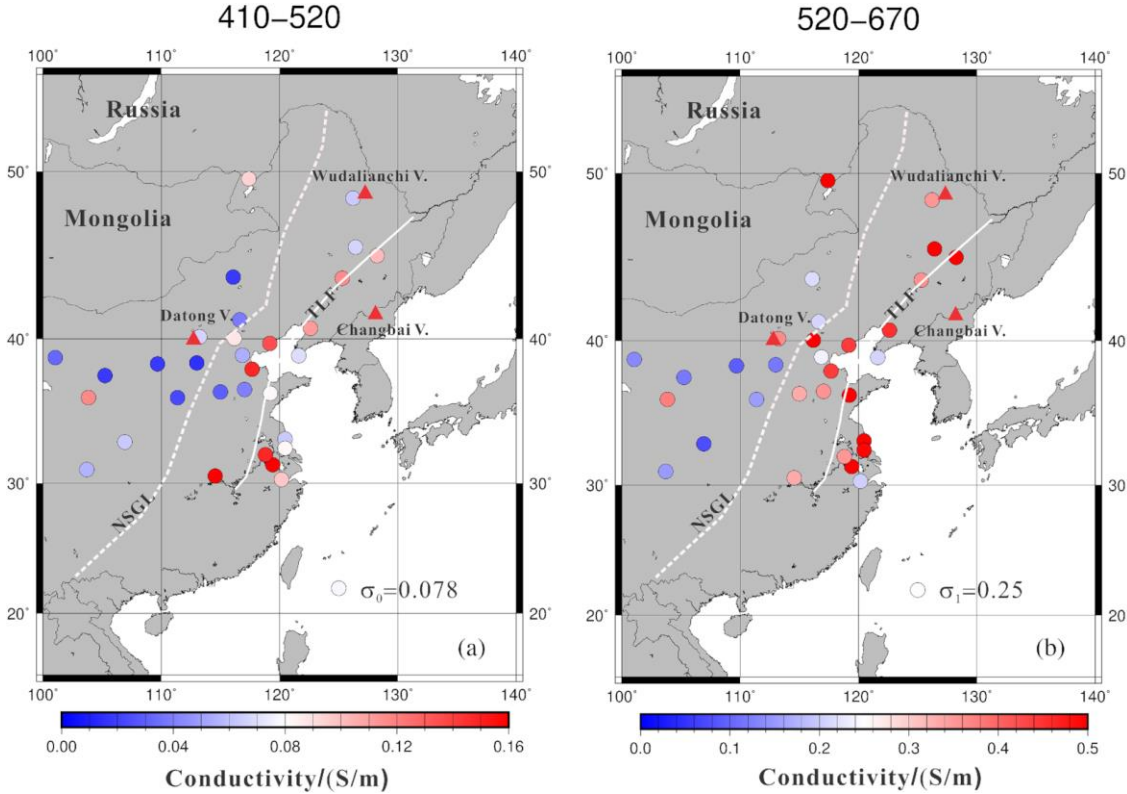
Shimizu et al. 2012



Matsuno et al. 2017

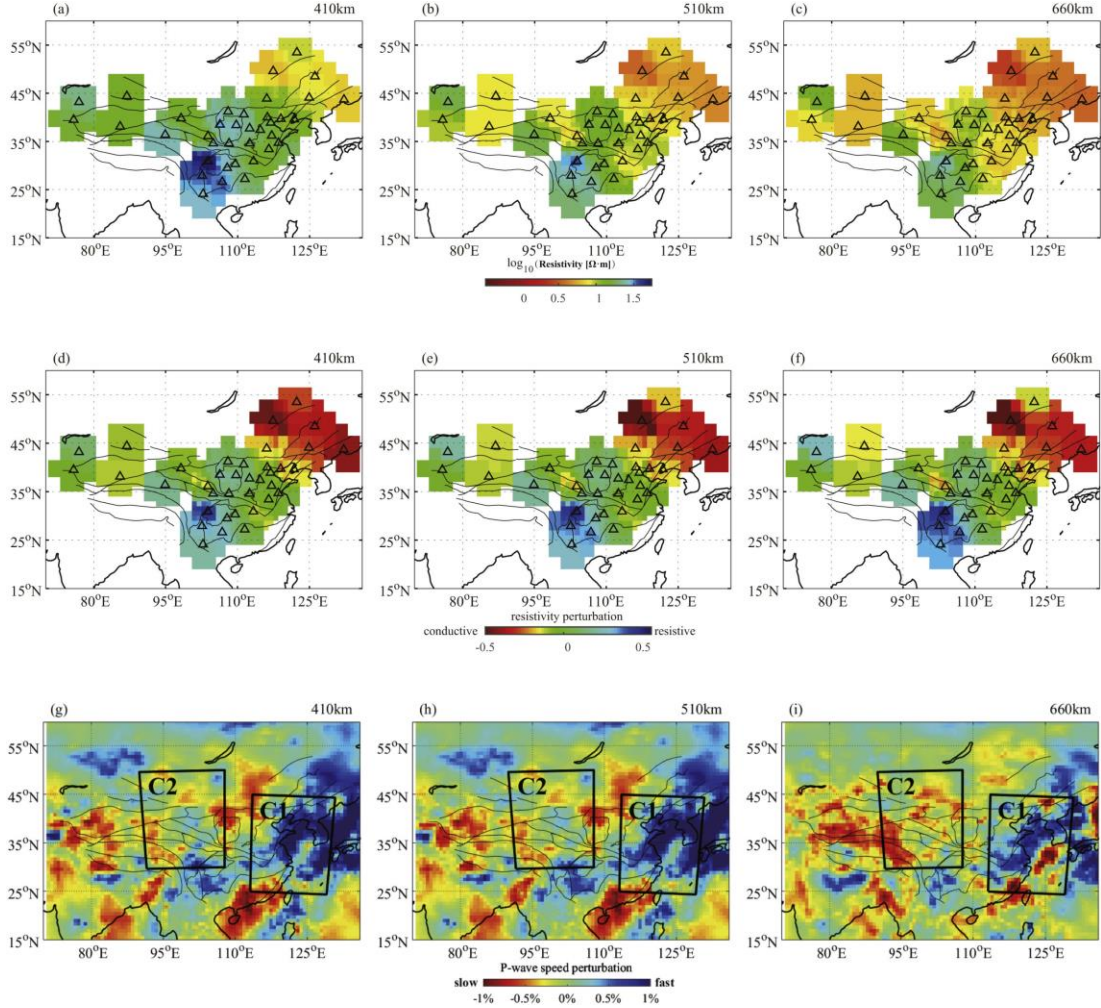
# Semi-global studies

Yuan et al. 2020



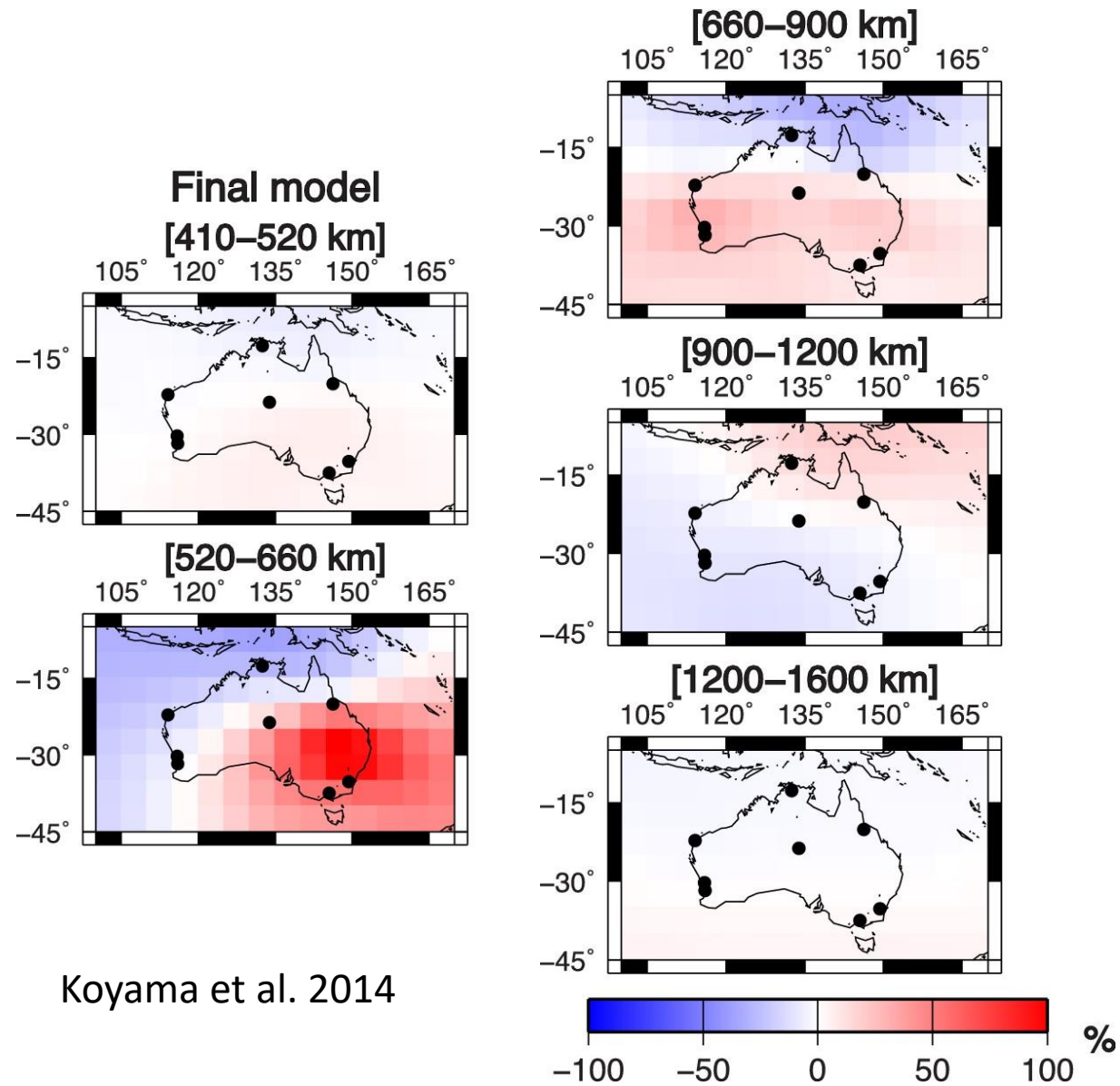
Zhang et al. 2020

*P10 source assumption*





# Semi-global studies



Koyama et al. 2014

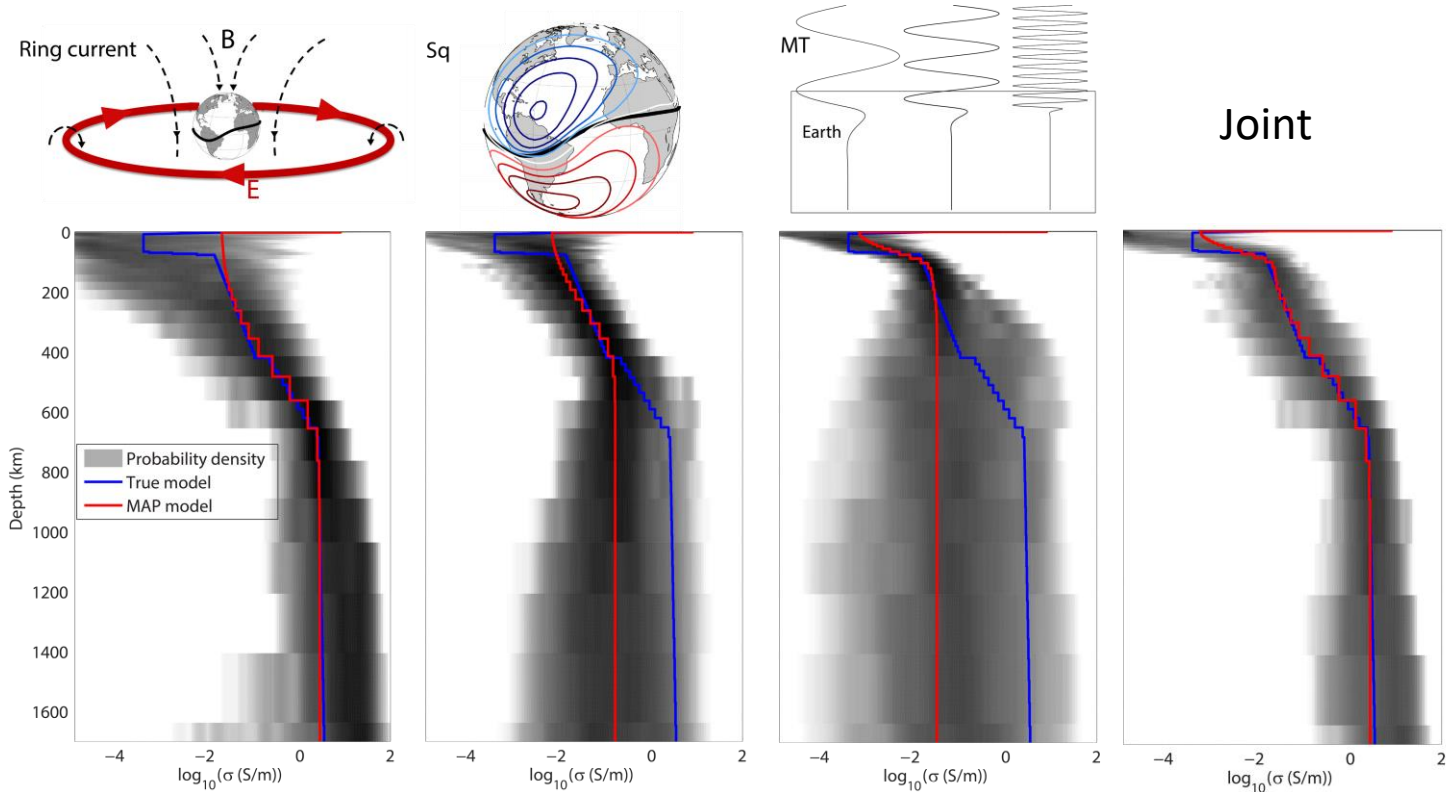
*P10 source assumption*

# Combining sources

$T > 1 \text{ day}$

$T = 4 \text{ hours} - 1 \text{ day}$

$T < 3 \text{ hours}$



Multi-source inversions:

- Matsuno et al. 2017: MT + RC
  - Grayver et al. 2017: Tides + RC
  - Zhang et al. 2019: Tides + MT
  - Munch et al. 2020: Sq + RC
  - Chen et al. 2022: MT + Sq + RC
  - Rigaud et al. 2022 (poster): MT + Sq + RC
- 
- All studies are 1-D (some with 3-D forward operator to model ocean/sediments)

# Conclusions and outlook

## Some highlights of the past decade

- Data:
  - Satellite constellations (Swarm + platform mags)
  - Regular large-scale ground arrays (US, AU, CN)
  - More often open data
- Modelling and inversion:
  - Modern parallel codes; multi-resolution grids; multi-source inversions
  - New 1D reference models, low-resolution global 3-D models.
- EM sources:
  - Oceanic tidal sources (we have data and tools)
  - New approaches for working with complex ionospheric/magnetospheric sources
  - Retirement of the Z/H method (*hard/impossible to discern source effects from conductivity variations in 3-D inversion*)

## Some challenges for next decade(s)

- Data:
  - Integrating satellite and ground observations
  - Still lack of (open) data...
- Modelling and inversion:
  - 3-D inversion of multi-source data (MT + global TFs + tides + Sq)
  - Interpretation: what do our models mean and what do we learn from them?
- EM sources:
  - Need to better understand external sources (build bridges to Magnetosphere/Ionosphere physics communities)